Optimal Planning and Scheduling of Battery Energy Storage Systems for Isolated Microgrids

by

Hisham Alharbi

A thesis
presented to the University of Waterloo
in fulfillment of the
thesis requirement for the degree of
Master of Applied Science
in
Electrical and Computer Engineering

Waterloo, Ontario, Canada, 2015

I hereby declare that I am the sole author of this thesis. This is a true copy of the thesis, including any required final revisions, as accepted by my examiners.

I understand that my thesis may be made electronically available to the public.

Abstract

Balancing the energy demand in isolated microgrids is a critical issue especially in the presence of intermittent energy sources. Battery Energy Storage Systems (BESS) can be installed in such circumstances to supply the demand and support the reserve requirements of the isolated microgrid. However, due to the high installation costs of BESS, there is a need for proper mechanisms to select such systems and size them optimally. Furthermore, since BESS are often installed to serve multiple applications, these should be properly modeled to coordinate their different functionalities.

In this thesis, a multi-year operational planning model is developed to determine the BESS optimal power rating and energy capacity along with the year of installation taking into account its coordinated operation. The model includes unit commitment formulation with renewable energy and BESS operational constraints. The optimal planning decisions are obtained for different BESS technologies under several scenarios of ownerships.

The uncertain patterns of solar and wind resources and system demand are considered and several microgrid operational scenarios are created. A stochastic optimization model is developed to determine the optimal BESS size and installation year including the different states of the uncertain microgrid variables. The stochastic optimization model is solved using a decomposition based two-stage iterative approach to cope with the large computational burden of such problems.

Acknowledgements

First and foremost, all praises are due to Allah the Almighty for giving me strength, knowledge, patience, and opportunity to accomplish this thesis.

Then, I would like to express my deepest thankfulness to my supervisor Professor Kankar Bhattacharya for his invaluable guidance, patience, kindness, and encouragement throughout the period of my Master's degree. My appreciation is also extended to Professor Claudio A. Cañizares and Dr. Amirhossein Hajimiragha for reviewing my thesis and providing their insightful comments and suggestions.

I would like to thank all the colleagues in the Power and Energy Systems Group at the University of Waterloo for their discussions and friendship. Also, I would like to thank my lab mates for providing such a pleasant work environment. Special thanks to Abdulaziz Almutairi, Abdullah Bin Humayd, and Walied Alharbi who have given me support and inspiration from the first stages of my graduate studies.

My sincere thanks go to my beloved parents Abdulrahman and Halima for their years of care and support. I would not have been able to get to this point in my academic career without their encouragement and prayers. May Allah reward them in this world and in the hereafter. I also would like to thank my brothers Hossam and Ahmed and my sister Raghad who encouraged me all the way.

I would never find the right words to express my gratitude to my lovely wife Mashael for her endless love, understanding, patience, and support. Her sacrifices allowed me to focus on my studies during the hard times we have passed through. Many thanks for her and for our little daughter Beesan for filling my life with happiness.

Finally, I wish to acknowledge the funding provided by Taif University to pursue my graduate studies, and the continued assistance from the Saudi Arabian Cultural Bureau in Canada.

Dedication

This thesis is dedicated to my parents, my wife, my daughter, and all my family.

Table of Contents

List of Tables

List of Figures

List of Abbreviations

BCF	Battery Capacity Factor
BESS	Battery Energy Storage System
BRF	Battery Reserve Factor
CAES	Compressed Air Energy Storage
DOD	Depth of Discharge
CHP	Combined Heat and Power
DG	Distributed Generator
EMS	Energy Management System
E/P	Energy to Power Ratio
FES	Flywheel Energy Storage
GA	Genetic Algorithm
HES	Hydrogen Energy Storage
Li-ion	Lithium-ion Batteries
MGO	Microgrid Operator
MILP	Mixed Integer Linear Programming
MINLP	Mixed Integer Non-linear Programming
NaS	Sodium Sulfur Batteries
NPV	Net Present Value
O&M	Operations and Maintenance
OPES	Optimal Power and Energy Sizing
PbA	Lead Acid Batteries
PCC	Point of Common Coupling
PHES	Pumped Hydro Energy Storage

PV	Photovoltaic
RES	Renewable Energy Sources
RR	Rate of Return
SMES	Superconducting Magnetic Energy Storage
SOC	State of Charge
UC	Unit Commitment
UCES	Ultra Capacitor Energy Storage
VRB	Vanadium Redox Flow Batteries

Nomenclature

Indices

s	Index for scenarios, $s = 1, 2, .., S$
y	Index for years, $y = 1, 2, .., Y_T$
h, q	Index for hours, $h = 1, 2, .., H; q = 1, 2, .., Q$
i	Index for DG, $i = 1, 2, .., I$
k	Index for sets of the DG's linearized cost function

Parameters

α	Discount rate (%)
β	Fuel cost escalation rate (%)
λ	Load growth rate (%)
RR	Rate of return (%)
ρ_s	Probability of scenario s
C^f	Fixed installation cost of BESS ($)
Cp^v	Variable installation cost of BESS associated with power rating ($/kW)
Ce^v	Variable installation cost of BESS associated with energy capacity ($/kWh)
OMC^f	Yearly fixed O&M cost of BESS ($/kW-year)
OMC^v	Variable O&M cost of BESS ($/kWh)
RC	Replacement cost of BESS ($/kW)
RY	Replacement year of BESS

θ_{dch}	Price of BESS discharge energy, purchased by microgrid (\$/kWh)
θ_{ch}	Price of energy at which BESS purchases from microgrid (\$/kWh)
θ_{res}	Price of reserves provided by BESS (\$/kW)
$\underline{Eff}_{ch}$, $\underline{Eff}_{dch}$	Charging/discharging efficiency (%)
$\overline{DOD}$	Maximum depth of discharge (%)
$\overline{EPR}$, $\underline{EPR}$	Maximum and minimum energy to power ratio
B_0	NPV of budget allocation in year-0 (\$)
B_{ITR}	NPV of budget allocation in year-0 of the iteration *ITR* (\$)
SU_i	Start-up cost of DG unit i (\$)
SD_i	Shut-down cost of DG unit i (\$)
a_i	Quadratic coefficient of cost function of DG unit i (\$/kWh^2)
b_i	Linear coefficient of cost function of DG unit i (\$/kWh)
c_i	Constant coefficient of cost function of DG unit i (\$)
$\overline{P}_i$	Maximum output power of DG unit i (kW)
$\underline{P}_i$	Minimum output power of DG unit i (kW)
$RampUp_i$	Ramp up limit of DG unit i (kW)
$RampDn_i$	Ramp down limit of DG unit i (kW)
$MinUp_i$	Minimum up-time of DG unit i (h)
$MinDn_i$	Minimum down-time of DG unit i (h)
G_i, L_i	Initial up-time or down-time required of DG unit i (h)
F_i^{min}	Generation cost of DG unit i at $\underline{P}_i$ (\$)
$Slope_{i,k}$	Slope of the linearized cost function of DG unit i in a certain set k
$Pset_{i,k}^{max}$	Maximum output power of DG unit i in a certain set k (kW)
$PV_{y,h}$	Forecasted PV output power (kW)
$Pw_{y,h}$	Forecasted wind output power (kW)
$Pd_{y,h}$	Forecasted demand (kW)
δ_{PV}	Error factor in forecasted PV (%)
δ_w	Error factor in forecasted wind (%)
δ_D	Error factor in forecasted demand (%)

M	Large number (assumed 10,000)
ε	Small number (assumed 1)

Variables

INS	NPV of installation cost of BESS ($)
OM	NPV of O&M cost of BESS ($)
MGOC	NPV of microgrid operational cost ($)
DCH REV	NPV of investor's revenue from BESS discharging ($)
Reserve REV	NPV of investor's revenue from BESS reserve provision ($)
CH Cost	NPV of BESS charging cost ($)
Wp_y	Power rating of BESS at year of installation and 0 otherwise (kW)
We_y	Energy capacity of BESS at year of installation and 0 otherwise (kWh)
P_{BESS}	Power rating of BESS (kW)
E_{BESS}	Energy capacity of BESS (kWh)
$PB_{y,h}$	BESS power; negative when charging, and positive when discharging (kW)
$SOC_{y,h}$	BESS state of charge (kWh)
Z_y	BESS installation decision, 1 or 0
Zc_y	BESS presence indicator, 1 or 0
$Zch_{y,h}$	Binary variable associated with BESS charging, 1 or 0
$Zdch_{y,h}$	Binary variable associated with BESS discharging, 1 or 0
$Pset_{i,k}$	Output power of DG unit i in a certain set k (kW)
$P_{y,h,i}$	DG output (kW)
$W_{y,h,i}$	Binary commitment decision of DG units, 1 or 0
$U_{y,h,i}$	Binary start-up decision of DG units, 1 or 0
$V_{y,h,i}$	Binary shut-down decision of DG units, 1 or 0
$RTH_{y,h,i}$	Reserve from DG units (kW)
$RB_{y,h,i}$	Reserve from BESS (kW)

Chapter 1

Introduction

1.1 Motivation

Microgrids are defined as small groups of customers and generating units which can be controlled independently and have the ability to manage the energy locally [1]. There are two modes of operation of microgrids: grid-connected and isolated mode, and each has a different energy management strategy [2]. One of the challenging problems in isolated microgrids is maintaining the balance between demand and supply. Since connection to the main grid is not available in isolated microgids, the integration of distributed generation (DG) sources such as photovoltaic (PV), wind, and other small-scale fuel-based units is essential in order to meet the demand.

Remote microgrids mainly depend on dispatchable DG units, such as diesel generators, since they can maintain the system reliability and operational flexibility in contrast to intermittent renewable energy sources (RES). For example, there are about 280 communities in Canada that have no access to the electric grid [3]. The total generation capacity in these microgrids is 615 MW, and the dominant source of energy is diesel generators; they account for more than 50% of

the total installed capacity, as shown in Figure 1.1.

The very high cost of fuel transportation in conjunction with environmental issues make the fuel-based DG units less favorable. According to [3], the minimum electricity tariff in these northern and remote communities of Canada, that depend on diesel generators, is as high as 0.45 $/kWh and even reaches 2.5 $/kWh in the arctic regions, while the average electricity tariff in the rest of Canada does not exceed 0.17 $/kWh. In order to circumvent this problem, there is a need for more integration of RES in such remote microgrid systems. However, RES are neither dispatchable nor predictable. Moreover, the high penetration of intermittent RES imposes technical problems because of the fluctuations in the output power which affects the power quality of microgids.

Energy storage systems provide a viable option in mitigating these problems. They help in meeting the load mismatch and facilitating integration of RES [4] via storing the extra energy from RES when demand is low and discharging the stored energy during peak load hours. Energy storage systems can be installed to serve the power system in many other applications as reported in [5]. In general, energy storage applications can be divided into two broad areas: energy management applications and power quality applications. Several energy storage technologies are available for use; however, some technologies may excel over others in some applications because of the different inherent characteristics, as shown in Figure 1.2 [6]. Amongst the various energy storage technologies, Battery Energy Storage Systems (BESS) have received significant attention over the last decade because of their role in improvement in system operational aspects and reduction in cost. BESS are also suitable for microgids because of their capability to be used for both energy management and power quality improvement applications. This is because of their fast response, options for different energy to power ratios, and compact size and mobility [7].

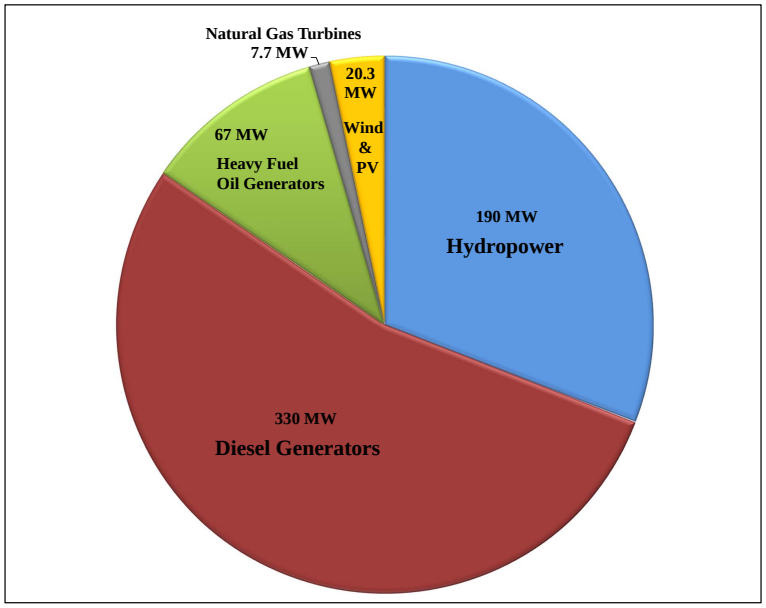

Figure 1.1: Share of generation sources in northern and remote communities of Canada [3]

The operational strategies of BESS differ from one application to another. Therefore, appropriate BESS technology, the optimal size, and the optimal operation strategy including charging/discharging cycles need to be chosen carefully, so as to result in the maximum benefit to the microgrid. To increase the benefit from BESS, more than one application can be synthesized at the same time; however, optimal sizing of such systems is a challenging problem.

In general, the larger the installed size of BESS, the greater is the improvement in microgid operations, in addition to a reduction in thermal generation costs. However, high installation cost (which includes the equipment cost and some associated fixed costs) is the main barrier to the wider deployment of BESS [8]. Therefore, the proper size of BESS need be determined in an operational-planning framework based on cost-benefit analysis to maximize the total microgid operational benefits at the least possible BESS installation cost.

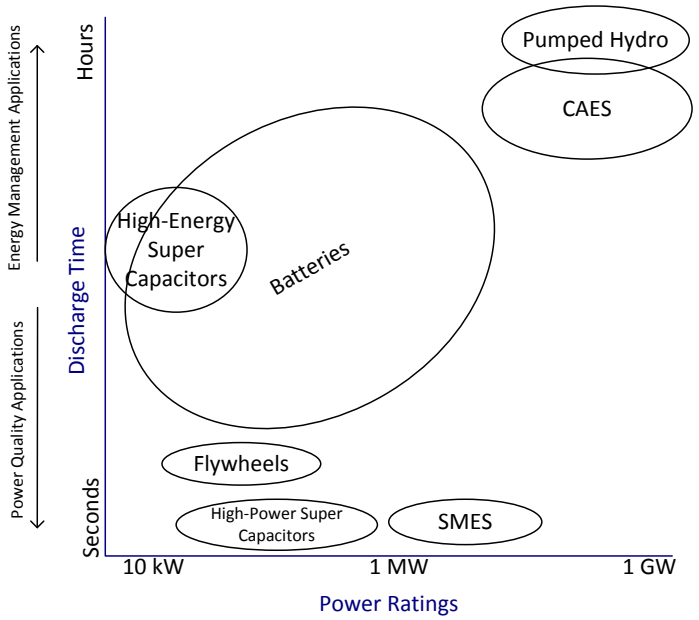

Figure 1.2: Energy storage technologies for different applications [6]

1.2 Literature Review

Several studies have been reported in the literature that address the problem of finding the optimal size of energy storage systems from different perspectives and in different applications.

The optimal power rating and energy capacity of BESS is determined in [9] for a hydrothermal power system using the multi-pass dynamic programming. The optimal size of BESS is determined based on maximizing the ratio of fuel cost savings to the capital cost of the installed BESS. In [10], the same approach is used to maximize the ratio of fuel cost savings over a 20 year period to the capital cost of BESS. A time-shift technique is used to find the initial values for the multi-pass dynamic programming which reduces the computation time. However, in the above papers, reducing the fuel cost by load leveling is the only application of BESS considered.

In [11], a heuristic approach to the unit commitment (UC) problem is developed and applied to a power system comprising thermal generators with several possible size combinations of BESS. Different applications of BESS such as spinning reserve, load leveling, and frequency control are studied. The BESS power and energy size corresponding to a specific application or a combination of applications that leads to maximum fuel cost savings, is considered the optimal solution for the problem.

Although the impact of the life-cycle cost of BESS is significant, it was not considered in [9–11]. The operations and maintenance (O&M) cost of BESS is considered in [12] when determining its optimal power and energy size. The model proposed in [12] aims to maximize the savings in production cost, distribution cost, and emission cost while minimizing the BESS life-cycle cost using the Tabu search optimization technique. The optimal capacity of BESS is determined in [13] using the objective of maximizing the net present value (NPV) of the total savings in distribution network costs taking into account the installation and O&M costs of BESS. The installed BESS is utilized in multiple applications in a distribution network. The optimization problem is solved using a non-dominated sorting genetic algorithm.

When a BESS is installed in a system that includes RES, it can be used for either energy management applications or power quality applications, as shown in Figure 1.3.

In one of the power quality applications of BESS [14] considering a PV/Battery system, the fluctuations of PV output power are mitigated by three methods including the installation of BESS. The optimal size of BESS is obtained to maximize the revenue generated from the PV/Battery system by reducing system fluctuations. The fluctuations of wind generation are taken into consideration for BESS sizing in [15] and [16]. The main objective of [15] is to find the optimal BESS size that maximizes the economic benefit while maintaining the output wind power constant. Also, the voltage across the DC link is required to be within a certain limit. However, since the capacity determined in [15] is based on peak wind generation, the

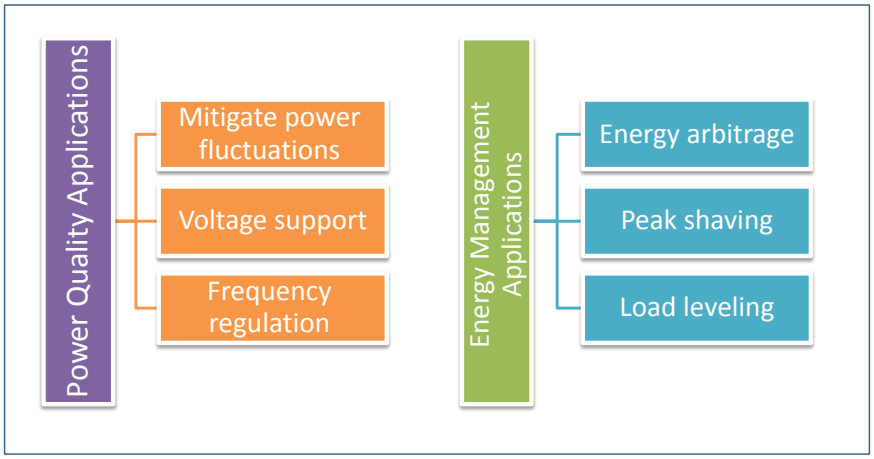

Figure 1.3: Energy storage applications with RES

determined BESS size may be higher than required. A stochastic optimization model is proposed in [16] to overcome this limitation and hence arrive at a more accurate BESS size to reduce power fluctuations from wind generation.

In the context of energy management applications, sizing BESS in a PV/Battery system is reported in [17] and [18]. Energy arbitrage and peak shaving applications are examined in [17] considering a PV/Battery system connected to the grid. The optimal size of BESS is determined so as to minimize the cost of net power purchased during peak hours as well as minimize the cost of capacity degradation after each discharging process, taking the advantage of time-of-use electricity pricing. Distributed BESS is also studied in a distribution system with high PV penetration in [18]. The optimal size of BESS is determined in [18], at each bus, based on a cost-benefit analysis, considering voltage regulation and peak load shaving applications.

In a wind-diesel isolated system [19], the optimal BESS size is determined so as to minimize the fuel and operating costs of the system over a 20-year planning period, while facilitating wind generation penetration. A two-stage approach is carried out to capture the wind variability and load uncertainty. Several scenarios are considered corresponding to different profiles of wind

and load. The first stage determines the BESS size that satisfies all scenarios while the second stage identifies the optimal operation, given the optimal size determined in the first stage.

Since a stand-alone wind generation system suffers from the unpredictability of output power, the optimal size of BESS that decreases the difference between the predicted and actual wind generation is investigated in [20]. The BESS size is determined to smoothen the output power fluctuations of the wind farm to within a range of ±4% of the forecast, for 90% of the operation period. The integration of wind generation in a system that lacks generation units for reserve, is studied in [21]. The BESS is installed to provide the reserve required for such a system. The optimal power rating and energy capacity are determined using temporal and non-temporal methods. Although savings in cost of reserves is achieved in the aforementioned studies, since BESS costs are not considered in [20] and [21], the proposed methods may lead to oversizing the BESS.

A similar application of BESS is discussed in [22] but with a flexible energy management strategy that allows curtailing the wind generation and selling energy when the price is low. The size of BESS is chosen based on a cost-benefit analysis in which the reduction in cost from installing BESS is more than the cost of the unserved energy. Similarly, optimal BESS size is determined to meet a certain specified level of power delivery from a wind farm in [23]. The difference herein with [22] is that, it selects the capacity of BESS based on the trade-off between lifetime and cost, including installation and O&M cost.

Another research examines the optimal BESS size and location in order to reduce the spilled wind energy [24]. The maximum spilled power and energy is used to determine the aggregated power and energy size of the installed BESS. The study is conducted from the perspective of utilities and DG owners to maximize their benefits based on cost-benefit analysis.

Hybrid systems which include both PV and wind generation are another thread of the literature on energy storage sizing. In the context of microgrids, sizing of energy storage is examined in [25] based on a cost-benefit analysis and unit commitment with spinning reserve considerations. The two microgrid operational modes, grid-connected and isolated, are studied and different BESS sizes for each mode are prescribed.

From another perspective, energy storage can be installed as a backup in order to increase the reliability of a critical system to the desired level [26]. The optimal size is determined in terms of power rating and energy capacity using an analytical approach to increase the availability or reduce the mean down time of supply to a critical load. The model is extended in [27] to an island-capable military microgrid with RES. Sequential Monte Carlo Simulation is used to analyze the system reliability. However, the installation cost of energy storage is not included in the proposed models. BESS sizing is proposed in [28] to enhance reliability in microgrids, wherein the BESS installation cost and its impact on the operating cost are considered. The optimization model is based on the UC formulation and solved as a mixed integer linear programming (MILP) problem. The power and energy size of BESS are determined to satisfy the reliability constraints in a grid-connected microgrid that comprises four thermal generators and a wind turbine. In [29], a two-stage stochastic model is proposed to determine optimal siting and sizing of BESS and help to increase the reliability of a distribution system to a level that the customer is willing to pay for. Siting and sizing of distributed BESS, along with a load shedding option are used to enhance the reliability. The optimal decisions are obtained using a genetic algorithm (GA) approach, based on a cost-benefit analysis.

In [30], an approach to optimize the size of different energy storage technologies including BESS based on power quality and energy management applications simultaneously is proposed for a system with high penetration of RES. Discrete Fourier transform is carried out to balance power in different time segments ranging from weeks to real-time. Each energy storage

technology is assigned a specific operational strategy during its time segment, and the size is determined based on the maximum energy storage requirement.

Several publications discuss optimizing DG capacity with BESS size. On the demand side of the grid, DG owners install BESS to decrease their consumption from the grid and utilize their hybrid systems as much as possible. For example, in [31], a method is proposed to find the optimal size of battery banks along with the number of PV modules to be installed in a stand-alone hybrid system to minimize the installation cost. The mismatch between the average output power of the PV and wind generation and the load determines the required BESS size. In [32], a GA based optimization model is proposed to select the number of components for a stand-alone PV/wind hybrid system including PV battery chargers. Sizing a wind-PV hybrid integrated system with battery bank is studied in [33]. The proposed sizing approach is based on factors such as deficiency of power supply probability, relative excess power generated, probability of un-utilized energy, and levelized energy cost. On a larger scale, the optimal DG size and BESS capacity is addressed in isolated and grid-connected wind-solar-battery hybrid systems in [34]. The proposed model minimizes the total cost while maintaining high power quality and system reliability considering the two modes of operation.

To consider the uncertain nature of RES, stochastic models are reported in [35] and [36] to optimize the size of DG and BESS. In household applications, a stochastic method based on Monte Carlo simulation and particle swarm optimization is proposed in [35]. The optimal size of wind generation and BESS is determined that minimizes the electricity cost for household customers considering the uncertainty in demand, electricity price, and wind generation. In [36], several capacities of energy storage systems, RES, diesel generators in isolated microgrids are considered in a joint optimization model. The large number of scenarios is handled by solving the model in a distributed optimization approach, which divides the problem into several sub-problems.

In view of the above discussions, there is a need to develop appropriate planning frameworks for determining the optimal power and energy size of BESS and optimal year of installation considering the long-term microgrid demand profile and presence of other energy resources. It is also important to consider uncertainty in demand and RES in the BESS planning framework.

1.3 Research Objectives

The main goal of the thesis is to develop an operational-planning framework for isolated microgrids to determine their optimal size of BESS to be installed and the optimal installation year over a planning horizon. The specific objectives of the thesis are stated as follows:

- Develop an optimization model for microgrids considering penetration of RES and dispatchable DG units. Different BESS technologies and their inherent characteristics and cost parameters are considered to arrive at the optimal selection of BESS technology in addition to the optimal power rating and energy capacity, and the optimal year of installation. The coordination between load leveling application and reserve support application of the BESS, to increase the benefit to the microgrid, is taken into account in the modeling framework. The reserve provided by BESS considers the three modes of operation: charging, discharging, and the standby mode, when providing reserve for a microgrid.

- Develop a stochastic programming model to capture the uncertainty of solar radiation, wind speed, and demand, using different probabilistic scenarios. Develop a decomposition-based approach to solve the stochastic programming model and hence determine the expected size of BESS, and the expected year of installation. The decomposition approach will be carried out in two stages: in the first, the power and

energy size of BESS will be determined, while in the second stage, the optimal year of installation is obtained.

- In conjunction with the above studies for BESS sizing, also determine and examine the optimal operational decisions of BESS and other microgrid resources.

1.4 Thesis Outline

The rest of the thesis is structured as follows: Chapter 2 presents the essential background on microgrids, energy storage technologies and their characteristics, and the generic UC formulation. In Chapter 3, the proposed optimization model for optimal planning of BESS, including determination of BESS size and year of installation, is discussed. Different BESS technologies are considered and several case studies considering isolated microgid operational requirements are carried out. The uncertainty of PV, wind, and load is incorporated and the model is further advanced to formulate a stochastic programming model, which is presented in Chapter 4. A two-stage decomposition approach is formulated to solve the stochastic programming model and hence determine the expected size and installation year of the BESS. Finally, a summary of the thesis, the main contributions, and the potential for future work are discussed in Chapter 5.

Chapter 2

Background

In this chapter, a brief background to the topics relevant to this thesis is presented. An overview of the microgrid concept is discussed in the first section. Then, energy storage systems including different technologies, aspects, and parameters are discussed. Finally, the mathematical model of the classical UC problem is presented.

2.1 Microgrids

The large-scale deployment of DG units in distribution systems has led to the development of the concept of microgrids. The microgrid system comprises a group of loads and small-scale sources of energy that operates as a single entity [1]. Each microgrid controls its resources to meet its demand at the distribution level. These resources include dispatchable DG units such as microturbines, fuel cells, and CHP generators, and RES such as hydro, PV and wind generation. In addition to these components, energy storage systems are essential elements in microgrids. Microgrids can operate as isolated systems and balance their demand via the available resources

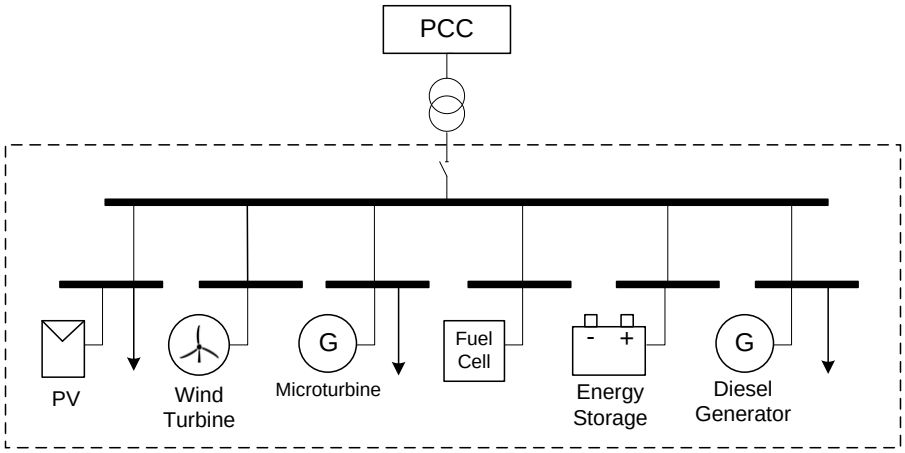

Figure 2.1: General microgrid layout

or they can be connected to the main grid at the point of common coupling (PCC) for bidirectional exchange of energy. A general microgrid layout is shown in Figure 2.1.

The characteristic of microgrids is different than the conventional power system since they have highly dynamic operations because of their dependency on DG units which are closer to the load [37]. Consequently, microgrids are usually equipped with the state-of-art power electronics, protection devices and reinforced by two-way communication systems in order to accommodate the generation resources at the distribution level and maintain the system reliability in presence of the bi-directional power flow. Controlling these components is performed by the microgrid's energy management system (EMS) which ensures optimizing the microgrid operation while ensuring reliability at least cost.

Although microgrids enhance the overall system efficiency, some operational challenges may face the microgrid operator (MGO) from the integration of intermittent resources, such as wind and solar. The fluctuations in output power from these resources have to be mitigated to ensure power quality and reliability standards in both grid-connected and isolated mode of operation. Some of the challenges in microgrids and the control strategies to overcome these issues are

discussed in [38].

The EMS in isolated microgrids is more challenging than in the grid-connected mode. Ensuring sufficient generation and scheduling resources based on the forecasted demand and availability of intermittent resources are important issues in isolated microgrids [39], [25]. The high uncertainty of RES adds another degree of complexity in maintaining the isolated microgrid's reliability. Moreover, the lack of rotational inertia from dispatchable generators requires additional sources and strategies to ensure the stability of the microgrid. On the other hand, the main aim in grid-connected mode of operation is maximizing the microgrid's benefit from exchanging energy with the main grid [40]. Therefore, each microgrid considers these issues in its EMS and optimizes its operation depending on the mode of operation.

Several demonstration projects have been conducted around the world to implement the concept of microgrid. In Canada, the integration of RES to electrify the northern and remote communities since the seventies decade can be considered as the beginning of implementing the microgrid concept. In the 1980s and 1990s, number of wind turbines and PV units with capacity of less than 60 kW and 5 kW respectively were installed to supply parts of the load in several isolated microgrids in conjunction with diesel generators [41]. More isolated microgrid projects have been developed afterwards such as the wind-diesel project in Ramea island in Newfoundland and Labrador. Six wind turbines with a total capacity of 395 kW have been installed to supply the Ramea isolated microgrid which has a peak demand of 1.2 MW [42]. Another example is the isolated microgrid in Kasabonika Lake First Nation community in Ontario. The microgrid demand is supplied by diesel generators and 60 kW of wind generation [43], [3]. In the Bella Coola remote microgrid in British Columbia, locally available hydro and diesel generation can effectively meet the entire microgrid demand. However, a combination of different energy storage technologies with an efficient EMS are utilized to optimize the power generation allocation [44].

The microgrid systems which are connected to the distribution system have also been implemented in Canada. For example, the Fortis-Alberta microgrid comprises 3.8 MW of wind generation and 3 MW of hydro generation to supply the load [45]. The microgrid is connected to the main grid and operates usually in grid-connected mode. However, in the case of faults, the microgrid may operate as an isolated system, or it can be connected to another temporary PCC [42]. The British Columbia Hydro Boston Bar system is another example of a grid-connected microgrid. The peak load in the microgrid is 3 MW which is supplied by the main grid in normal cases at the PCC, which is the 69-kV/25-kV substation [42]. During the isolated mode, the microgrid is supplied by a hydro plant of 8.64 MW. In Quebec, a 15 MW load is connected normally to the Hydro Quebec distribution system via a 125-kV line. The microgrid is supplied by 31 MW thermal generation units in isolated mode [42].

2.2 Energy Storage Technologies

A wide range of energy storage technologies exist today. In general, energy storage technologies are classified into two categories based on the form of the stored energy: direct energy storage and indirect energy storage technologies [46]. The former store the energy as electrical energy and do not require any conversion to other forms. In contrast, the indirect energy storage technologies require converting electrical energy from/to mechanical energy or chemical energy. Technologies of each type are presented in Figure 2.2.

2.2.1 Direct Energy Storage Technologies: Electro-magnetic

This type of energy storage technologies includes Superconducting Magnetic Energy Storage (SMES) and Ultra Capacitor Energy Storage (UCES). These technologies are developed versions

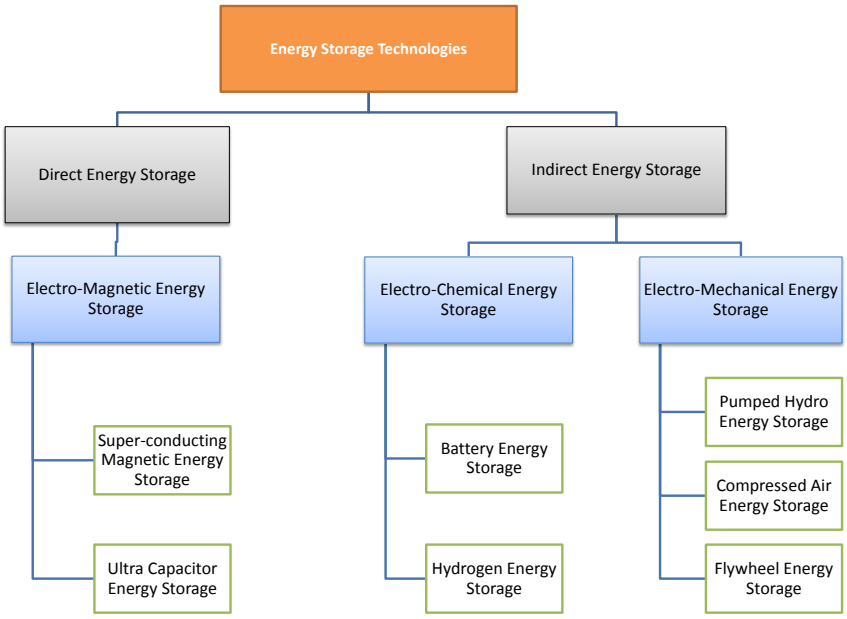

Figure 2.2: Classification of energy storage technologies [46]

of the basic electrical devices: inductors and capacitors, respectively. They have the capability to discharge high large quantities of power within a very short time. Therefore, they fit best in power quality applications [46].

2.2.2 Indirect Energy Storage Technologies: Electro-mechanical

The mechanical energy storage technologies store the energy in the form of kinetic energy or potential energy. The technologies of this type include Pumped Hydro Energy Storage (PHES), Compressed Air Energy Storage (CAES), and Flywheel Energy Storage (FES).

2.2.2.1 Pumped Hydro Energy Storage (PHES)

This is one of the earliest large-scale energy storage technologies. During low demand periods, the charging energy is used by motors to pump water to a higher level reservoir. When energy is required to be discharged, water is released to a lower reservoir, and the potential energy of the released water is used to operate a hydroelectric turbine and generate electrical energy. PHES is used for energy management applications because of its high energy capacity and low energy cost. However, the geographic and environmental restrictions limit the installing of PHES in some cases. Also, despite the low cost of energy, the fixed installation cost of PHES is very high and requires longer time for cost recovery as compared with other technologies, which makes PHES less attractive [6]. For these reasons, PHES may not be a feasible option for microgrids.

2.2.2.2 Compressed Air Energy Storage (CAES)

The other mature energy storage technology is the Compressed Air Energy Storage (CAES). In the charging process, the CAES system compresses air in a special reservoir, and during discharging, the compressed air is expanded by heating and then passed through a turbine to generate electrical energy. There are two types of CAES based on the design of the compressed air reservoir, underground or aboveground. The aboveground CAES does not require geologic specifications and uses tanks or on-site pipes as a reservoir for the compressed air [5]. On the other hand, the underground CAES stores the compressed air in an underground geologic formation such as salt caverns, aquifers, and depleted natural gas fields. The installation cost of the aboveground CAES is higher than the underground CAES since the later depends on natural reservoir which reduces the unit cost of energy significantly. For the same reason, the capacities and discharge time of the aboveground design are less. The aboveground CAES capacity is typically within 3-50 MW range with discharge time of 2 to 6 hours, whereas the underground

CAES is capable to store up to 400 MW with maximum discharge time of 26 hours depending on the available size of the geologic formation [6]. Because of the site requirements and the scale of energy capacities, the aboveground CAES is more suitable for microgrid applications than the underground CAES.

2.2.2.3 Flywheel Energy Storage (FES)

FES stores energy in a rotating shaft as kinetic energy. To charge the FES, electrical energy is used to rotate it and the rotation speed of the shaft is proportional to the stored energy. Therefore, when FES discharges, the kinetic energy is converted to electrical energy via the generator and the rotation speed decreases as FES discharges. FES is useful for power applications because of its fast response time [6]. However, although FES has high power capability and fast response, its limited energy capacity to few kWh limits its use in large scale applications [6].

2.2.3 Indirect Energy Storage Technologies: Electro-chemical

Electrical energy can be stored in the form of chemical energy. There are two different concepts of electro-chemical energy storage, first includes all the battery technologies, including flow batteries, while the second is a recent development, Hydrogen Energy Storage (HES).

2.2.3.1 Battery Energy Storage Systems (BESS)

The scope of this thesis is to focus on BESS because of their maturity level and their range of application to system level issues in a microgrid. Therefore, the four main BESS technologies will be discussed with their technical characteristics.

Sodium Sulfur Batteries (NaS):

Several studies have been conducted to develop this technology, especially in Japan. At the current time, NaS BESS is only available at energy to power (E/P) ratios ranging from 6 to 7 [5]. Therefore, it has the capability to discharge for more than 6 hours at rated power. In addition, the relatively high round-trip efficiency and their long cycle life make them more valuable in energy management applications. Moreover, NaS BESS has a capability to discharge at 5 times its rated power for a few minutes to meet transient fluctuations in power, which is a significant feature of the batteries in power quality applications [5].

NaS BESS also have high energy and power density [6] and does not suffer from self-discharge effect [47]. Consequently, because of all these advantages, this technology is considered as a mature technology and has been used in several grid-scale applications. However, because NaS BESS operation requires high temperature, there are some concerns about their safety [47].

Vanadium Redox Flow Batteries (VRB):

VRB BESS is a battery from the *flow batteries* family. It was first introduced in the 1970s [48]. Since power rating of these batteries depends on the size of the cell stack, while the volume of the electrolyte determines the energy capacity, VRB BESS has no E/P ratio constraints [47].

The cycle life of VRB BESS is significantly high and does not depend on the depth of discharge (DOD) [6]; hence, their lifetime is usually measured by calendar life. One of the features of VRB BESS is that the power stack can be adjusted to the desired level, and the power rating can be changed to suit the application, either it is power quality application such as voltage regulation or energy management application such as energy arbitrage [48]. Researchers are working on reducing the power density of these batteries which is one of their drawbacks.

Lead Acid Batteries (PbA):

PbA BESS are one of the most developed and mature batteries in the world, and widely used in

several applications since they were introduced in the early 1860s [5]. The limitations of PbA BESS include their low power and energy density, and reliability. Also, PbA BESS have low cycle life compared to other batteries. Despite these limitations, PbA BESS can be used in power applications or energy applications because of their noticeable low cost and high efficiency, beside their maturity level [47].

Lithium-ion Batteries (Li-ion):

The research on Li-ion BESS was started in the 1960s [49]. They have been used in small-scale energy storage applications for several decades and recently in large-scale applications, especially in the automotive sector.

The advantages of Li-ion BESS include their very high efficiency, high cycle life and fast response time. However, Li-ion BESS are expensive compared to the other types of batteries because of their protection and insulation requirements [50].

Since their E/P ratio is usually less than unity, Li-ion BESS are typically used in power applications. Furthermore, it is projected that Li-ion BESS of typical size 50 kW can have a discharge time of less than 4 hours by 2015 [6], and consequently, it can also be used for some energy management applications.

2.2.3.2 Hydrogen Energy Storage (HES)

HES technology is a new concept of electro-chemical energy storage. It is based on converting the electrical energy to hydrogen and oxygen via an electrolyzer. The hydrogen is stored and then used in discharging mode to generate electrical energy using a fuel cell. HES has high energy density and long cycle life. However, the round-trip efficiency of HES is very low as compared with BESS [47].

2.3 Energy Storage Systems

In order to address the differences between the various energy storage technologies and their applications, the most important properties of energy storage systems need be understood.

2.3.1 Power and Energy Size, E/P Ratio

Unlike electrical generators, energy storage systems are not infinite sources of energy. Therefore, the size of an energy storage system is identified by its rated power and the maximum energy that can be stored.

The power size of an energy storage system is defined as the rate at which the energy storage is capable of discharging/charging power continually. In normal operation, the maximum injected/drawn power is the nameplate rating of the system, however, some types of energy storage have the ability to discharge more power than their rated value for a short period during contingency situations. Also, in most technologies, the charge rate is usually less than the discharge rate.

The energy size represents the maximum amount of energy that can be stored for a certain time. The capacity is expressed usually in kWh or MWh. It can also be represented in Ah when the voltage across the energy storage is not assumed to be fixed.

The relationship between the power and energy size for a certain energy storage technology is known as the E/P ratio, and it is defined as follows:

$$E/P = \frac{\text{Energy Capacity, } kWh}{\text{Power Rating, } kW} \tag{2.1}$$

For example, in energy storage systems used for power quality applications, the E/P ratio is

usually less than unity since the maximum discharge/charge power is more important than the energy capacity. On the other hand, energy storage systems used in energy management applications have an E/P ratio more than unity due to the need for large energy capacity.

2.3.2 Discharge Time

It is the maximum duration for which the energy storage can discharge at rated power, and is expressed as follows:

$$\text{Discharge Time} = \frac{\text{Available Energy Capacity, } kWh}{\text{Power Rating, } kW} \tag{2.2}$$

It is to be noted that while discharge time depends on the available energy capacity or the DOD, the E/P ratio considers the entire energy capacity. In other words, if the energy storage is allowed to utilize its full capacity, then the discharge time equals the E/P ratio, otherwise, the discharge time is always less than the E/P ratio.

The discharge time and E/P ratio of an energy storage technology varies over a range as shown in Figure 1.2, and depicts the range of applications that storage systems can be utilized for. The energy storage systems that have low discharge time (seconds to few minutes) are more suitable for power applications, while systems with high discharge times (several minutes to hours) are better in energy management applications.

It has to be mentioned that some technologies, such as batteries, have a wider range of E/P ratio than others, which make them better suited for both power quality and energy management applications.

2.3.3 Lifetime

Most energy storage technologies suffer from degradation which affects their performance and reduce their lifetime. Three major factors affect the lifetime, and whenever one of them reaches its limit, the energy storage system should be replaced.

(a) *The calendar lifetime (years):* depending on the technology, after certain years of installation, the energy storage may not operate efficiently, even though it may not have operated frequently.

(b) *Number of cycles (cycles):* when the number of charging/discharging cycles reaches its maximum, the energy storage system should be replaced. This factor is critical in applications requiring frequent shallow charge/discharge cycles.

(c) *Total discharged energy (kWh or MWh):* in applications that require deep charging and discharging cycles, the total discharged energy determines the lifetime of energy storage.

To reduce the impact of degradation, the operation of energy storage system should be controlled to increase its benefit at least cost. For example, in energy management applications, where the discharged energy determines the lifetime, the energy storage may not be allowed to discharge beyond a certain level of its energy capacity. The maximum discharge limit is expressed as the DOD of energy storage (%). It is noted that the level of energy to which the energy storage is charged is known as state of charge (SOC), expressed in kWh in this thesis. Accordingly, the DOD of energy storage is defined as follows:

$$DOD(\%) = \frac{\text{Energy Capacity} - \text{Minimum SOC Level}}{\text{Energy Capacity}} \times 100 \tag{2.3}$$

Reducing the DOD has a significant impact on prolonging the lifetime of the energy storage system [48]. However, a low value of DOD requires installing a larger size of energy storage. Therefore, balancing the two factors is important to reduce the total energy storage cost.

2.3.4 Round-Trip Efficiency

The loss of energy due to the conversion from grids to energy storage systems and vice versa is represented by the round-trip efficiency. It is the amount of energy that can be discharged from energy storage for a given amount of energy charged. In some cases, the charging efficiency associated with energy conversion in charging process is different than the discharging efficiency. The round-trip efficiency is the multiplication of both of them. Energy storage technologies have different range of round-trip efficiencies. Higher efficiency of a certain technology might be available but at higher cost.

2.4 The UC Problem

The UC problem aims to find the optimal commitment schedule of the available generation resources over a period of time to meet the demand taking into account the characteristics of generating units and other power system constraints [51]. The optimal commitment schedule in UC problems yields the least operation cost. Several optimization techniques and algorithms for solving the UC problem have been discussed in [51] and [52]. The generic UC mathematical model is presented below:

2.4.1 Objective Function

Minimize the total operation cost of generating units over a period of time:

$$MIN \quad J = \sum_{h=1}^{H} \sum_{i=1}^{I} (F_i(P_{h,i})W_{h,i} + SU_i U_{h,i} + SD_i V_{h,i}) \tag{2.4}$$

The cost function of the thermal generators at any hour is generally given as follows:

$$F_i(P_i) = a_i P_i^2 + b_i P_i + c_i \quad \forall i \tag{2.5}$$

where a, b, and c are the cost coefficients of each generating unit in \$/kW^2, \$/kW, and \$, respectively. Because of the nonlinearity of the cost function, the Piecewise Linear Upper Approximation Method [53] is used in this thesis in order to formulate the UC model as a MILP problem. In this method, the quadratic cost function in (2.5) is divided into sets of linear functions and formulated as follows:

$$F_i(P_i) = F_i^{min} W_i + \sum_k Slope_{i,k} Pset_{i,k} \quad \forall i, \forall k \tag{2.6}$$

where the minimum cost F_i^{min} and the slope of each set $Slope_{i,k}$ are constants and can be obtained from the following relations:

$$F_i^{min} = a_i(\underline{P_i})^2 + b_i(\underline{P_i}) + c_i \quad \forall i \tag{2.7}$$

$$Slope_{i,k} = \frac{[F_i(Pset_{i,k}^{max}) - F_i(Pset_{i,k-1}^{max})]}{[Pset_{i,k}^{max} - Pset_{i,k-1}^{max}]} = a_i(Pset_{i,k}^{max} + Pset_{i,k-1}^{max}) + b_i \quad \forall i, \forall k \tag{2.8}$$

The total output power of a generating unit considering all the sets is as follows:

$$P_i = \sum_k Pset_{i,k} \qquad \forall i \tag{2.9}$$

The output power bounds of each set are given as:

$$0 \leq Pset_{i,k} \leq (Pset_{i,k}^{max} - Pset_{i,k-1}^{max})W_i \qquad \forall i, \forall k \tag{2.10}$$

2.4.2 Constraints

Demand Supply Balance: This constraint ensures sufficient generation is available to meet the demand at each hour.

$$\sum_{i=1}^{I} P_{h,i} = Pd_h \qquad \forall h \tag{2.11}$$

Reserve Requirements: The available capacity of committed generators has to meet certain reserve requirement. It is assumed that the reserve should be at least 10% of the demand at each hour.

$$\sum_{i=1}^{I} (\overline{P_i} W_{h,i} - P_{h,i}) \geq 0.1 Pd_h \qquad \forall h \tag{2.12}$$

Generating Unit Limits: Each generating unit has upper and lower bounds on its power production, as follows:

$$\underline{P_i} W_{h,i} \leq P_{h,i} \leq \overline{P_i} W_{h,i} \qquad \forall i, \forall h \tag{2.13}$$

Ramp Up/Down Constraints of Generating Units: The intra-hour increase/decrease in generation satisfies the ramping limits of generating units, as follows:

$$P_{h,i} \leq P_{h-1,i} + RampUp_i \qquad \forall i, \forall h; h \neq 1 \tag{2.14}$$

$$P_{h,i} \geq P_{h-1,i} - RampDown_i \qquad \forall i, \forall h; h \neq 1 \tag{2.15}$$

Minimum Up Time Constraints of Generating Units: When a generating unit is turned on, it must not be de-committed before satisfying its minimum up time. These constraints are formulated as in [54].

$$\sum_{h=1}^{G_i} (1 - W_{h,i}) = 0 \qquad \forall i \tag{2.16}$$

$$\sum_{q=h}^{h+MinUp_i-1} W_{q,i} \geq MinUp_i[W_{h,i} - W_{h-1,i}] \qquad \forall i, h = G_i + 1, ...H - MinUp_i + 1 \tag{2.17}$$

$$\sum_{q=h}^{H} [W_{q,i} - (W_{h,i} - W_{h-1,i})] \geq 0 \qquad \forall i, h = H - MinUp_i + 2, ...H \tag{2.18}$$

Minimum Down Time Constraints of Generating Units: When a generating unit is turned off, the minimum down time should be satisfied before committing it. The constraints are formulated as follows [54]:

$$\sum_{h=1}^{L_i} W_{h,i} = 0 \qquad \forall i \tag{2.19}$$

$$\sum_{q=h}^{h+MinDn_i-1} (1 - W_{q,i}) \geq MinDn_i[W_{h-1,i} - W_{h,i}] \qquad \forall i, h = L_i + 1, ...H - MinDn_i + 1 \tag{2.20}$$

$$\sum_{q=h}^{H} [1 - W_{q,i} - (W_{h-1,i} - W_{h,i})] \geq 0 \qquad \forall i, h = H - MinDn_i + 2, ...H \tag{2.21}$$

Generating Units Binary Coordination: To ensure proper coordination between the generator status and the start-up/shut down binary variables, the constraint is formulated as below:

$$U_{h,i} - V_{h,i} = W_{h,i} - W_{h-1,i} \qquad \forall i, \forall h \tag{2.22}$$

2.5 Summary

The chapter introduces some essential background topics required for this thesis. A brief discussion about the microgrid concept, different modes of operations and operation challenges are first presented. In the second section, the state-of-art energy storage technologies, systems and their important properties and parameters are discussed. Finally, the basic MILP model to solve the UC problem is presented.

Chapter 3

Optimal Selection and Sizing of BESS

In this chapter, a mathematical model is developed that seeks to obtain the optimal power and energy ratings of a BESS in an isolated microgrid, and the optimal year of installation within the planning horizon. It is noted that the planning study considers only the installation of BESS, while dispatchable DG units and RES are considered to be existed in the microgrid under study. The proposed model is based on a UC formulation with some modifications to accommodate BESS installation decision variables. Different structures of BESS ownership are considered, as follows:

- MGO owns and schedules the BESS.
- Third-party (investor) owns the BESS and schedules it from its own perspective.

3.1 Mathematical Modeling Framework

3.1.1 Energy Storage System Applications

As discussed earlier, energy storage system applications can be classified into two general categories: power quality and energy management applications. These can also be divided into five service provisions to the grid, as shown in Table 3.1. These applications can be synthesized to provide as much benefit to the grid as possible. However, some technical and operational conflicts may prevent the energy storage system to be used in certain applications simultaneously [5]. For example, the energy storage system that supports the reserves should not be assigned to other applications that require frequent discharging cycles. Consequently, two new parameters are introduced in this thesis that measures the performance of the BESS, as follows:

$$\text{BESS Capacity Factor } (BCF) = \frac{\text{Total Energy Discharged by BESS, } kWh}{\text{Total Energy Demand, } kWh} \tag{3.1}$$

$$\text{BESS Reserve Factor } (BRF) = \frac{\text{BESS Reserve Contribution, } kW}{\text{Total Required Reserve, } kW} \tag{3.2}$$

3.1.2 Charging and Discharging Energy in BESS

BESS discharged energy is the total released energy from the battery to the microgrid before accounting for its discharging efficiency. It quantifies the actual usage of BESS in computing the variable O&M cost, charging cost, and discharging revenue. Although charging cost and discharging revenue are related to the drawn/injected energy from/to the microgrid, discharged energy can be used with considering BESS efficiency to determine the total drawn and injected

Table 3.1: Classification of energy storage system applications [6]

Bulk Energy Services	Electric Energy Time-shift (Arbitrage)
	Electric Supply Capacity
Ancillary Services	Area Regulation
	System Reserves
	Voltage Support
	Black Start
	Load Following/Ramping Support for Renewables
	Frequency Response
Transmission Systems	Transmission Upgrade Deferral
	Transmission Congestion Relief
	Transmission Support
Distribution Systems	Distribution Upgrade Deferral
	Voltage Support
Customer Energy Management Services	Power Quality
	Reliability
	Retail Energy Time-Shift
	Demand Side Management

energy. All these quantities can be expressed using one variable that is already defined: the BESS power (PB). Figure 3.1 shows the energy loss in BESS because of the BESS efficiency during charging and discharging process, while the standby loss is not considered. Because the initial and final SOC are set to be at the same level in one operation day, the energy loss in that day can be expressed as follows:

$$BESS\ Energy\ Loss = Total\ Energy\ Drawn\ (A) - Total\ Energy\ Injected\ (D) \tag{3.3}$$

Since the BESS power in charging mode is negative, and the total charging energy is greater than the total discharging energy, the total energy loss in the BESS can be given as follows:

$$BESS\ Energy\ Loss = \sum_{h} (-PB_h\ \Delta h) \tag{3.4}$$

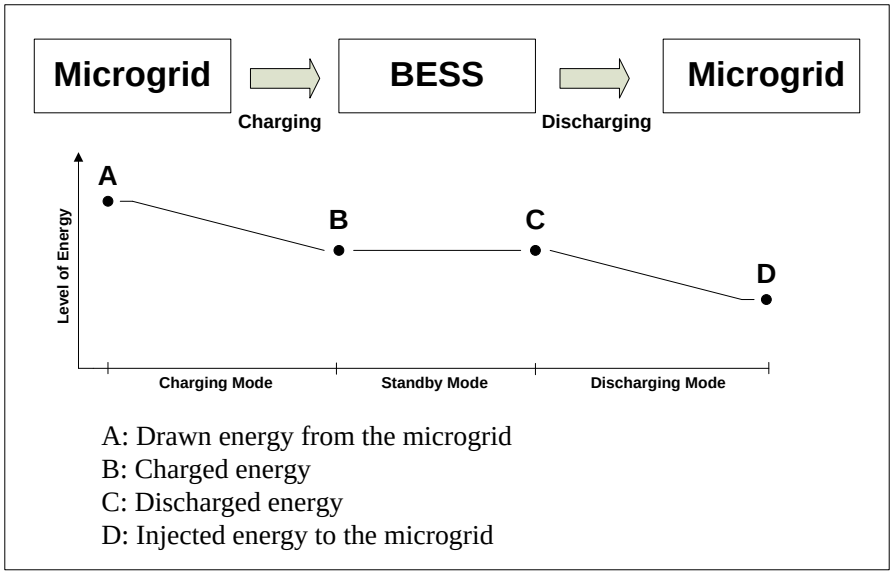

Figure 3.1: Energy losses because of the charging and discharging efficiency

From Figure 3.1, the following relations can be obtained:

$$\textit{Total Energy Drawn } (A) = \frac{\textit{Total Energy Injected } (D)}{Eff_{ch} Eff_{dch}} \tag{3.5}$$

$$\textit{Total Energy Discharged } (C) = \frac{\textit{Total Energy Injected } (D)}{Eff_{dch}} \tag{3.6}$$

Hence, the total energy drawn, discharged, and injected can be expressed respectively as follows:

$$\textit{Total Energy Drawn } (A) = \frac{1}{1 - Eff_{ch} Eff_{dch}} \sum_{h=1}^{H} (- PB_h \, \Delta h) \tag{3.7}$$

$$\textit{Total Energy Discharged } (C) = \frac{Eff_{ch}}{1 - Eff_{ch} Eff_{dch}} \sum_{h=1}^{H} (- PB_h \, \Delta h) \tag{3.8}$$

$$\textit{Total Energy Injected } (D) = \frac{Eff_{ch} Eff_{dch}}{1 - Eff_{ch} Eff_{dch}} \sum_{h=1}^{H} (- PB_h \, \Delta h) \tag{3.9}$$

where Δh is assumed to be one hour. Note that in (3.7)-(3.9), it is inherently assumed that the efficiencies of charging and discharging are always less than 100%. In ideal BESS, A, B, C, and D are at the the same level.

3.1.3 BESS Ownership Structures

This thesis considers two different ownership structures of the BESS as discussed next. It will be noted that the objective functions are significantly different as the ownership of BESS changes because of differing perspectives of the cost.

3.1.3.1 BESS Owned and Scheduled by MGO

In this model, the MGO installs BESS to meet the increase in demand of the microgrid over the long term. The objective is to minimize the NPV of the total cost which includes BESS installation cost (*INS*), BESS O&M cost (*OM*), and the microgrid operational cost (*MGOC*).

$$J_1 = INS + OM + MGOC \tag{3.10}$$

The *INS* cost component of BESS comprises costs proportional to the installed power rating ($/kW) and energy capacity ($/kWh), and a fixed installation cost ($) irrespective of the size:

$$INS = \sum_{y=1}^{Y_T} \Big[\frac{1}{(1+\alpha)^y} (Cp^v Wp_y + Ce^v We_y + C^f Z_y) \Big] \tag{3.11}$$

The *OM* cost component comprises the fixed cost, variable cost, and replacement cost. The fixed and replacement costs are proportional to the BESS power rating, whereas the variable cost depends on the discharged energy from the BESS.

$$
\begin{aligned}
OM = & \sum_{y=1}^{Y_T} \Big[\frac{1}{(1+\alpha)^y} OMC^f P_{BESS_y} \Big] \\
& + 365 \times \sum_{y=1}^{Y_T} \sum_{h=1}^{H} \Big[\frac{1}{(1+\alpha)^y} \, OMC^v \, (\frac{Eff_{ch}}{1 - Eff_{ch} Eff_{dch}})(-PB_{y,h}) \Big] \\
& + \Big[\frac{1}{(1+\alpha)^{RY}} + \frac{1}{(1+\alpha)^{2RY}} + ... \Big] \, RC \, P_{BESS_{y=1}} \\
& + \sum_{y=RY+1}^{Y_T} \Big[\Big(\frac{1}{(1+\alpha)^y} + \frac{1}{(1+\alpha)^{y+RY}} + ... \Big) \, RC \, \Big(P_{BESS_{y-RY+1}} - P_{BESS_{y-RY}} \Big) \Big]
\end{aligned}
\tag{3.12}
$$

The first term of Equation (3.12) represents the fixed O&M cost of the BESS. In the second term, the total energy discharged is used to compute the variable O&M cost. Since the model considers one typical day per year, the variable cost is extrapolated to one year using a factor of 365. The replacement cost of BESS is applied when the BESS's years of operation reach its predefined life *RY*. The third term of (3.12) denotes the replacement cost for a BESS installed in the first year, while the last term represents the replacement cost if it is installed after the first year. The replacement cost may apply several times if the BESS life is reached more than once over the planning horizon.

The *MGOC* component represents the operational cost of dispatchable DG units including their start-up and shut-down cost, taking into account the annual fuel cost escalation. The generation cost of one typical day in a year is extrapolated to represent the cost of the corresponding year.

$$
MGOC = 365 \times \sum_{y=1}^{Y_T} \sum_{h=1}^{H} \sum_{i=1}^{I} \Big[\frac{1}{(1+\alpha)^y} \Big[(1+\beta)^{y-1} F_i(P_{y,h,i}) W_{y,h,i} + SU_i U_{y,h,i} + SD_i V_{y,h,i} \Big] \Big] \tag{3.13}
$$

where $F_i(\cdot)$ is the operational cost function of a DG.

3.1.3.2 BESS Owned and Scheduled by Third-Party (Investor)

This model investigates the benefit accrued to a third-party from installing BESS, with the objective to maximize the profit from the energy supplied to the microgrid. The investor is expected to bear the BESS installation cost and the O&M cost. Also, since the BESS is assumed to be owned by a third party, the only way to charge the batteries is to purchase energy from the microgrid. Fixed charging and discharging energy prices are assumed in this model, θ_{ch} and θ_{dch} respectively, considering a higher discharge price to generate profit. Since this is an isolated microgrid, electricity market prices do not apply, and it is assumed that the MGO and investor have contractual agreements for θ_{ch} and θ_{dch}. The revenue from discharging and cost of charging can be expressed as a function of the BESS discharge energy. The BESS can help in the provision of microgrid's reserve at fixed price θ_{res}. Since the model is carried out from the investor's point of view, it is assumed that the BESS owner has the right to balance the demand based on the most profitable UC schedule to the investor. However, the microgrid is responsible for the thermal generation cost. As mentioned earlier, the model considers one typical day per year, and hence the discharging and reserve revenue as well as the charging cost are extrapolated to represent the revenue/cost of one year using a factor of 365. The installation cost and O&M cost are similar to the first model, but rate of return (RR) for an investor is considered instead of the discount rate.

$$J_2 = (DCH\ REV + Reserve\ REV) - (CH\ Cost + INS + OM) \tag{3.14}$$

$$DCH\ REV = 365 \times \sum_{y=1}^{Y_T} \sum_{h=1}^{H} [\frac{1}{(1+RR)^y}\ \theta_{dch}\ (\frac{Eff_{ch}Eff_{dch}}{1-Eff_{ch}Eff_{dch}})(-PB_{y,h})] \tag{3.15}$$

$$Reserve\ REV = 365 \times \sum_{y=1}^{Y_T} \sum_{h=1}^{H} [\frac{1}{(1+RR)^y}\ \theta_{res}\ RB_{y,h}] \tag{3.16}$$

$$CH\ Cost = 365 \times \sum_{y=1}^{Y_T} \sum_{h=1}^{H} [\frac{1}{(1+RR)^y}\ \theta_{ch}\ (\frac{1}{1 - Eff_{ch}Eff_{dch}})(-PB_{y,h})] \tag{3.17}$$

where *INS* is defined as follows:

$$INS = \sum_{y=1}^{Y_T} \Big[\frac{1}{(1+RR)^y}(Cp^v Wp_y + Ce^v We_y + C^f Z_y)\Big] \tag{3.18}$$

The *OM* is formulated as:

$$\begin{aligned} OM = & \sum_{y=1}^{Y_T} \Big[\frac{1}{(1+RR)^y} OMC^f P_{BESS_y}\Big] \\ & + 365 \times \sum_{y=1}^{Y_T} \sum_{h=1}^{H} \Big[\frac{1}{(1+RR)^y}\ OMC^v\ (\frac{Eff_{ch}}{1 - Eff_{ch}Eff_{dch}})(-PB_{y,h})\Big] \\ & + \Big[\frac{1}{(1+RR)^{RY}} + \frac{1}{(1+RR)^{2RY}} + ...\Big]\ RC\ P_{BESS_{y=1}} \\ & + \sum_{y=RY+1}^{Y_T} \Big[\Big(\frac{1}{(1+RR)^y} + \frac{1}{(1+RR)^{y+RY}} + ...\Big)\ RC\ \Big(P_{BESS_{y-RY+1}} - P_{BESS_{y-RY}}\Big)\Big] \end{aligned} \tag{3.19}$$

3.1.4 Model Constraints

3.1.4.1 Demand-Supply Balance

The demand-supply balance shall include RES and BESS. This constraint ensures sufficient generation from dispatchable DG units and RES to meet the demand at an hour. The demand is assumed to increase annually by a constant rate, λ.

$$\sum_{i=1}^{I} P_{y,h,i} + PB_{y,h} + PV_{y,h} + Pw_{y,h} = (1+\lambda)^{y-1} Pd_h \qquad \forall y, \forall h \tag{3.20}$$

3.1.4.2 Dispatchable DG Units Constraints

The dispatchable DG units constraints are similar to the ones presented in Chapter 2, and given by constraints (2.13) to (2.22) with considering the year index y.

3.1.4.3 Microgrid Reserve Requirements

The MGO ensures a minimum reserve level of 10% of the demand plus factors accounting for uncertainty in demand and RES forecasting errors [25], [55]. The reserve constraint is modeled as follows:

$$RTH_{y,h} + RB_{y,h} \geq (0.1 + \delta_D)(1 + \lambda)^{y-1} Pd_h + \delta_{PV} PV_{y,h} + \delta_W Pw_{y,h} \qquad \forall y, \forall h \tag{3.21}$$

$$RTH_{y,h} \leq \sum_{i=1}^{I} (\overline{P_i} W_{y,h,i} - P_{y,h,i}) \qquad \forall y, \forall h \tag{3.22}$$

$$RB_{y,h} \leq -PB_{y,h} + \min\left\{[SOC_{y,h} - E_{BESS_y}(1 - \overline{DOD})]Eff_{dch}, P_{BESS_y}\right\} \qquad \forall y, \forall h \tag{3.23}$$

As shown in (3.21), RB is the reserve from BESS that supports the spinning reserve from DG units; denoted by RTH, and given by (3.22) in providing reserves for the microgrid. In (3.23), the BESS reserve contribution is defined either by its available energy (SOC), accounting for discharging efficiency, or its power rating. The lower value of the two, determines the maximum reserve that can be provided by the BESS. Note that, for the sake of dimensions, the available energy (SOC) and E_{BESS} (given in kWh) are considered for a one hour interval, thereby making them equivalent to be as a kW basis. The committed charging and discharging power of the BESS is included in modeling the BESS reserve. When the BESS is discharging, it supplies a portion of the demand, and hence the discharged power should not be reconsidered as reserve. However, the BESS can discharge part of its energy and use the remaining as reserve. In case of

charging, the charging power can be used as a reserve since the BESS can interrupt its charging instantaneously, which allows the DG that is committed to supply the BESS, to be used for supplying demand instead.

It is worth mentioning that upward and downward reserves are required in systems with high penetration of RES to ensure maintaining the variations in RES generation and demand [56]. In this thesis, the RES generation is assumed to be always less than the microgrid demand, and hence only upward reserve is considered.

3.1.4.4 BESS Size Constraints

Power Size of BESS

In order to allow the model to optimize the power size of the BESS, the following constraints are considered:

$$P_{BESS_y} = Wp_y \quad ; y = 1 \tag{3.24}$$

$$P_{BESS_y} = Wp_y + P_{BESS_{y-1}} \quad \forall y; y \neq 1 \tag{3.25}$$

$$Wp_y \geq Z_y \quad \forall y \tag{3.26}$$

$$Wp_y \leq M\, Z_y \quad \forall y \tag{3.27}$$

To keep the linearity of the model, two variables are defined for BESS power size, P_{BESS_y} and Wp_y. The first denotes the power rating of BESS, and once the BESS is installed, it remains constant over the plan horizon. On the other hand, while Wp_y also denotes the installed BESS size, it is used to compute the installation cost, and is active only at the year of installation; otherwise, it is zero, as per (3.24). The constraints (3.26) and (3.27) are used to activate the binary variable Z_y when installing BESS using the big M method.

Energy Size of BESS

Similar to the power rating, two variables are defined for energy capacity E_{BESS_y} and We_y. The following constraints are considered:

$$E_{BESS_y} = We_y \quad ; y = 1 \tag{3.28}$$

$$E_{BESS_y} = We_y + E_{BESS_{y-1}} \quad \forall y; y \neq 1 \tag{3.29}$$

$$We_y \geq Z_y \quad \forall y \tag{3.30}$$

$$We_y \leq M\, Z_y \quad \forall y \tag{3.31}$$

Energy to Power Ratio (E/P)

As mentioned in Chapter 2, the energy capacity of the BESS for a certain power rating, is determined based on its E/P ratio, as follows:

$$\underline{EPR}\, P_{BESS_y} \leq E_{BESS_y} \leq \overline{EPR}\, P_{BESS_y} \quad \forall y \tag{3.32}$$

$\overline{EPR}$ and $\underline{EPR}$ are the maximum and minimum possible E/P ratio for a certain BESS technology. The E/P ratio constraint also determines the maximum discharge time at rated power, as discussed in Chapter 2.

Coordination of Binary Variables

To ensure limiting the activation of the binary variable associated with the BESS installation, to only once over the planning horizon, the following constraint is considered:

$$\sum_{y=1}^{Y_T} Z_y \leq 1 \tag{3.33}$$

Budget Constraint

The NPV of the BESS installation cost should not exceed the NPV of the allocated budget for the year.

$$INS \leq B_0 \tag{3.34}$$

3.1.4.5 BESS Operational Constraints

BESS Power and SOC Relationship

The relationship between the charging and discharging power of BESS and its SOC can be described as follows:

$$\frac{PB_{y,h}}{Eff_{dch}} Zdch_{y,h} + PB_{y,h} Eff_{ch} Zch_{y,h} = SOC_{y,h} - SOC_{y,h+1} \quad \forall y, \forall h; h \neq 24 \tag{3.35}$$

However, the equation (3.35) is not linear; therefore, the charging and discharging constraints are formulated in [57] to linearize it using the big M method.

(a) *Charging constraints:*

$$-PB_{y,h} Eff_{ch} - M\, Zdch_{y,h} \leq SOC_{y,h+1} - SOC_{y,h} \quad \forall y, \forall h; h \neq 24 \tag{3.36}$$

$$SOC_{y,h+1} - SOC_{y,h} \leq -PB_{y,h} Eff_{ch} + M\, Zdch_{y,h} \quad \forall y, \forall h; h \neq 24 \tag{3.37}$$

(b) *Discharging constraints:*

$$\frac{-PB_{y,h}}{Eff_{dch}} - M(Zch_{y,h} - Zdch_{y,h} + 1) \leq SOC_{y,h+1} - SOC_{y,h} \quad \forall y, \forall h; h \neq 24 \tag{3.38}$$

$$SOC_{y,h+1} - SOC_{y,h} \leq \frac{-PB_{y,h}}{Eff_{dch}} + M(Zch_{y,h} - Zdch_{y,h} + 1) \quad \forall y, \forall h; h \neq 24 \tag{3.39}$$

Since (3.36)-(3.39) do not force the binary variables $Zch_{y,h}$ and $Zdch_{y,h}$ associated with charging and discharging respectively, to be activated during the process, the following constraints are also considered:

$$-M\ Zch_{y,h} \leq PB_{y,h} \qquad \forall y, \forall h \tag{3.40}$$

$$M\ Zdch_{y,h} \geq PB_{y,h} \qquad \forall y, \forall h \tag{3.41}$$

Initial and Final SOC

The initial and final SOC of the BESS are assumed to be 50% of the installed BESS energy capacity. The initial SOC is formulated as follows:

$$SOC_{y,h} = 0.5\ E_{BESS_y} \qquad \forall y, h = 1 \tag{3.42}$$

Similarly, (3.36)-(3.39) are adopted to the desired final value of SOC, i.e.,

$$SOC_{y,h+1} = 0.5\ E_{BESS_y} \qquad \forall y, h = 24 \tag{3.43}$$

Limits on BESS Power and SOC

The limits on BESS power and SOC are formulated respectively, as follows:

$$-P_{BESS_y} \leq PB_{y,h} \leq P_{BESS_y} \qquad \forall y, \forall h \tag{3.44}$$

$$(1 - \overline{DOD})E_{BESS_y} \leq SOC_{y,h} \leq E_{BESS_y} \qquad \forall y, \forall h \tag{3.45}$$

The minimum SOC limit is set based on the maximum DOD of the BESS. For example, if the DOD is 80%, the minimum SOC level is 20% of the energy size.

Coordination of Binary Variables

This constraint ensures that simultaneous charging and discharging of the BESS does not take place. Also, it ensures that there is no charging or discharging if the binary variable associated with BESS installation (Z_y) has not been activated yet.

$$Zch_{y,h} + Zdch_{y,h} \leq \sum_{1}^{y} Z_y \qquad \forall y, \forall h \tag{3.46}$$

Optimizing the BESS power and energy ratings and year of installation is formulated as a MILP problem in the proposed models (3.10) to (3.46), and they are solved in GAMS using CPLEX solver.

3.2 Results and Analysis

3.2.1 Microgrid Test System

The proposed model is applied to the modified CIGRE medium voltage microgrid [39] to determine the optimal BESS plan. The controllable generating units in the microgrid are three diesel generators, one combined heat and power (CHP) diesel, and one CHP microturbine with a total capacity of 5,510 kW. The DG data shown in Table 3.2 are taken from [39]. The installed PV capacity is 840 kW, and wind capacity is 1,450 kW.

The planning period in the case studies is 10 years. Forecasted demand and RES generation profile, that comprises wind and solar PV, for one typical day are inputs to the model, as shown in Figure 3.2 and Figure 3.3, respectively. The peak demand of the microgrid in the first year is 5,290 kW, and is assumed to increase annually by 1%. The fuel cost is considered to increase by 3% every year [48]. The discount rate considered in the planning is 8%.

The microgrid is required to maintain an operating reserve equivalent to 10% of its hourly demand plus a certain fraction of the forecasted RES generation and demand, to account for forecasting error. The forecasting error parameters δ_D, δ_{PV}, and δ_W are assumed to be 3%, 9%, 13%, respectively [25].

Four BESS technologies are examined, namely, NaS, VRB, PbA, and Li-ion BESS. The performance and cost parameters of different BESS technologies, shown in Table 3.3, are taken from [6]. The fixed installation cost, applicable to all technologies, is assumed to be $20,000. The maximum size for BESS is assumed as, P_{BESS} = 6,500 kW, and E_{BESS} = 6,500 kWh, the options are considered to be available in multiples of 50 kW and 50 kWh, respectively.

Table 3.2: Dispatchable DG parameters [39]

i#	Generator Type	$\overline{P}$ (kW)	$\underline{P}$ (kW)	a ($/kWh^2)	b ($/kWh)	c ($)	SU ($)	SD ($)
1	Diesel Generator	800	350	0	0.2881	7.5	15	5.3
2	CHP Diesel	310	60	0	0.2876	0	7.35	1.44
3	Diesel Generator	1400	600	0	0.2571	25.5	45	8.3
4	Diesel Generator	2500	1000	0.00001	0.224	45.5	95	15.3
5	CHP Microturbine	500	100	0.0318	1.8	6	0.27	0

3.2.2 BESS Owned and Scheduled by MGO

This ownership structure model is studied considering three scenarios associated with different microgrid operational requirements, as follows:

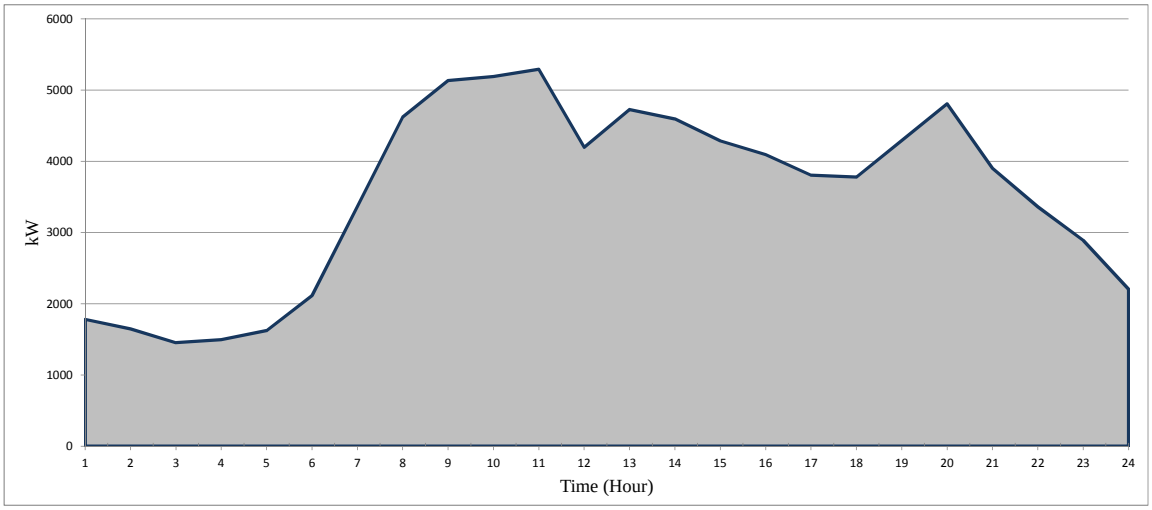

Figure 3.2: Demand profile for a typical day of the first planning year

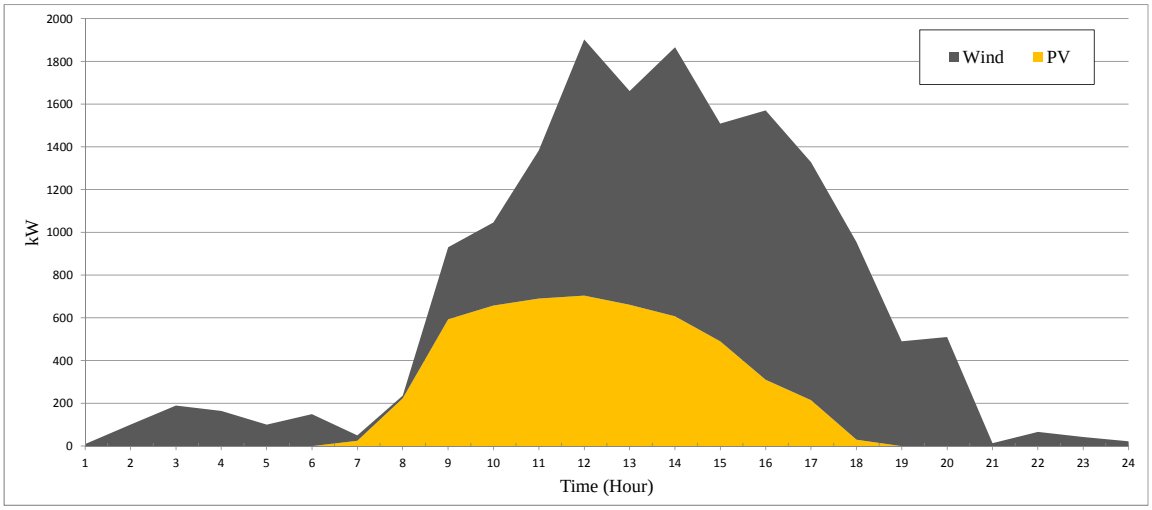

Figure 3.3: RES generation profile for a typical day of the first planning year

Table 3.3: BESS performance and cost parameters [6]

BESS Type	NaS	VRB	PbA	Li-ion
Cp^v (\$/kW)	757	2133	1407	1859
Ce^v (\$/kWh)	372	880	275	901
OMC^f (\$/kW-year)	9.2	16.5	26.8	13.2
OMC^v (\$/Wh)	0.8	1.6	1.1	1.4
RC (\$/kW)	0	720	375	1560
RY (y)	15	8	8	5
Charging efficiency	87%	83%	95%	95%
Discharging efficiency	87%	83%	95%	95%
Maximum DOD	80%	100%	80%	100%
E/P ratio range	6-8	N/A	1-5	1-4

3.2.2.1 Scenario 1: Adequate Generation Available for Secure Operation

In this scenario, generation from DG units along with the forecasted RES are at a level that allows the microgrid's net generation to meet the demand and reserve requirements without the need for BESS in the entire planning horizon. Therefore, BESS is not assigned to discharge or support reserves at any specific hours. Nevertheless, BESS may be installed to improve the microgrid operation via leveling the load to avoid starting up expensive generators during peak demand hours and by providing reserves.

Optimal values of BESS types are shown in Table 3.4. Note the small size of BESS selected for all the types, because the microgrid generation is adequate, and the operation is secure (with adequate reserves).

The microgrid operational cost before installing BESS is \$59,833,790 (*not in table*), and a reduction in this cost as well as in the total cost is achieved with any BESS technology, as shown in Table 3.4. The lowest cost is obtained for PbA followed by NaS, VRB, and then Li-ion

BESS. In this scenario, the difference in microgrid operational cost across the BESS types is not significant, and therefore the BESS installation and O&M costs impacts the optimal selection of the BESS technology. For example, although the largest reduction in microgrid operational cost is observed when installing Li-ion BESS, the high installation cost and O&M cost increases the total cost and makes Li-ion BESS the last option.

All the BESS types are selected for installation in the second year because the benefits from installing in the first year is not larger than the reduction in NPV from deferring the installation. The selected power rating of 500 kW is the same for all BESS. However, the energy capacity differs based on the E/P constraints, efficiency, and the maximum DOD.

Table 3.4: Optimal installation decisions and related costs in Scenario 1

BESS Type	NaS	VRB	PbA	Li-ion
Year of Installation	Year 2	Year 2	Year 2	Year 2
P_{BESS}	500 kW	500 kW	500 kW	500 kW
E_{BESS}	3000 kWh	650 kWh	700 kWh	550 kWh
INS	\$1,298,440	\$1,421,896	\$785,322	\$1,238,897
OM	\$26,651	\$228,279	\$172,087	\$530,292
$MGOC$	\$54,376,027	\$54,413,735	\$54,383,656	\$54,368,266
Total Costs	\$55,701,117	\$56,063,909	\$55,341,065	\$56,137,455

The overall operation of all the BESS technologies and their effect on the microgrid operation follows almost the same pattern. Therefore, for the sake of conciseness, the operation of PbA BESS is highlighted in Figure 3.4, which presents the supply-demand balance, and Figure 3.5, which shows the reserve requirements, for a typical day in year 10. The net generation before BESS is installed represents the forecasted RES and the total capacity of the DGs, while after installing the BESS, the net generation excludes the power drawn to charge the BESS. In this scenario, the net generation before installing BESS is adequate to meet the demand. Likewise, the reserve provided by DG units is shown before and after installing the BESS. The reserve

capacity available from DG units can maintain the security of microgrid operation. It is noted from Figures 3.4 and 3.5 that there is a sudden increase in required reserve at hour 8 and a rapid drop at hour 20 in year 10. The BESS power and energy ratings are governed by the reserve requirements at hour 8. The contribution of the BESS to the reserve of the order of 485 kW at this hour helps in avoiding starting up an expensive DG unit.

From Figure 3.4, it is noted that the microgrid demand is somewhat levelized by charging the BESS during the periods of relatively low demand and discharging when there is an increase in demand. The BESS should be fully charged before hour 8 to provide the required reserve; therefore, it is charged during the early hours, when the committed generation capacity is adequate to charge the BESS along with meeting the demand. Since the final SOC of the BESS should be as the initial state (50%), the BESS discharges the extra stored energy in an optimal manner. This pattern also applies to VRB, and Li-ion BESS with slight differences. However, for NaS BESS, the specified lowest E/P ratio of 6 requires an energy capacity at least of 3000 kWh. Considering an initial SOC of 50% and discharge efficiency of 87%, the available energy for discharge is 783 kWh, which is sufficient to meet the reserve requirement of 485 kW at the critical hour 8 without the need for charging the BESS. Over and above, it can provide 298 kW of power to meet the demand. However, the discharge of 298 kW is not sufficient to alter DG schedules or reduce the microgrid operational cost at any hour, and hence the NaS BESS remains idle during the entire day. It is noted from the studies that the BCF for VRB, PbA, and Li-ion BESS in year 10 are 0.25%, 0.45%, and 0.26%, respectively.

As noted from Figure 3.5 and additional studies, all BESS technologies provide reserves during the hours 7-11, 13-15, 19-22, and 24. The amount of reserve provided differs depending on the installed size of the BESS and the available energy, as well as the strategy of discharging and charging. For example, NaS BESS provides more reserve than other BESS technologies since the stored energy is kept as reserve, while the DG units are used to supply the demand.

Consequently, NaS BESS has the largest BRF amongst all the types, which is 36% in year 10, while VRB, PbA, and Li-ion BESS have 30%, 26%, and 30%, respectively. It also can be noticed that the PbA BESS is used more in load leveling than in providing reserves, compared to other BESS technologies.

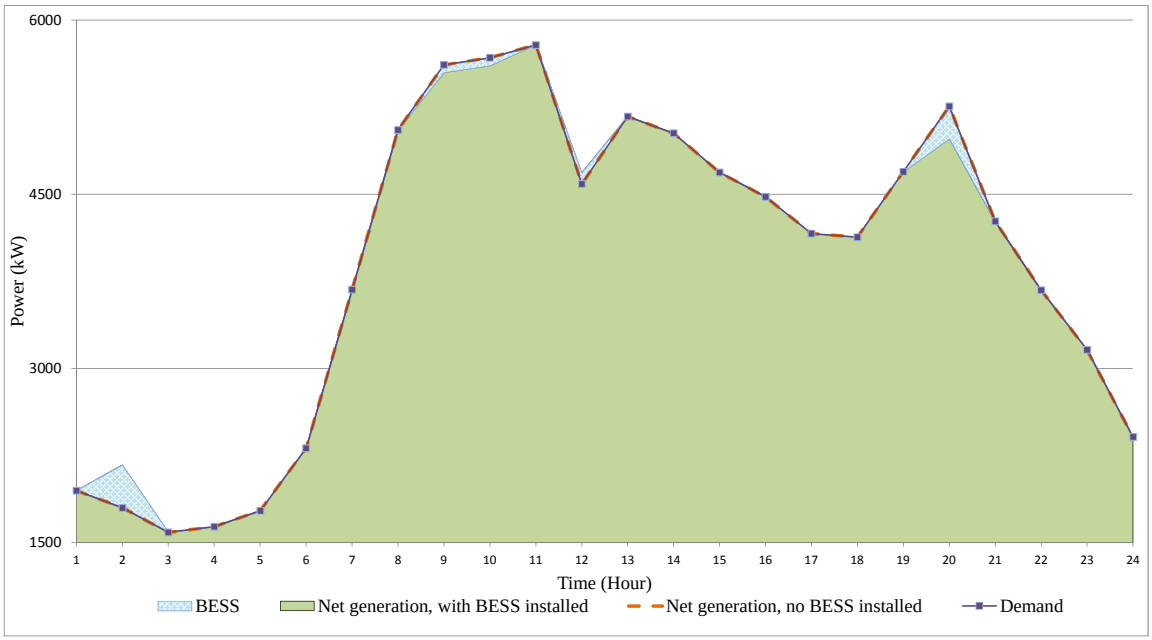

Figure 3.4: Supply and demand of year 10 in Scenario 1 (PbA BESS)

3.2.2.2 Scenario 2: Adequate Microgrid Generation with Unsecure Operation

In this scenario, a case is examined where the microgrid net generation without BESS is sufficient to supply the demand but does not satisfy the reserve requirements. The RES profile is assumed to be reduced by 50%. The BESS is required to be installed since the DG reserve capacity cannot meet the reserve requirements. As mentioned earlier, the BESS that is used in reserve support application may not be required to discharge as long as the reserve is not used. However, BESS

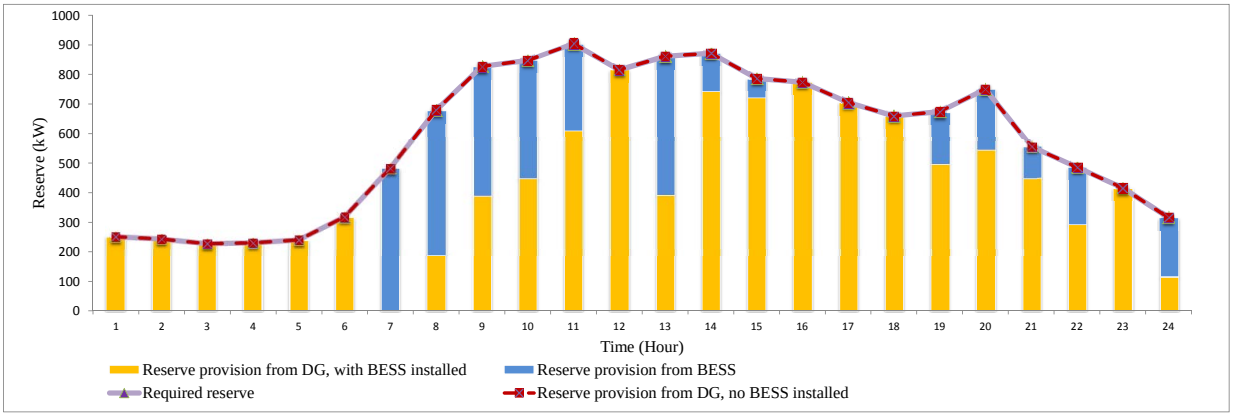

Figure 3.5: Reserve of year 10 in Scenario 1 (PbA BESS)

can be used for load leveling if its operation does not conflict with the main aim, which is to support the system reserve.

The reserve is required to be supported by the BESS at hours 8-11 and 20. The size of the installed BESS should be at least sufficient to provide reserve at hours when DG units cannot provide the required reserve. However, the optimal size can be increased to save microgrid operational cost by load leveling, as in the first scenario.

The main results of this scenario are presented in Table 3.5. As expected, the optimal size of all the BESS technologies are larger than those in Scenario 1 because of the increase in microgrid operational requirements.

The microgrid operational cost without installing BESS is $67,843,870 (*not in table*), but the reserve constraint however is not satisfied, starting from the third year. The selected BESS reduces the cost and helps the microgrid to meet its required reserves. Installing PbA BESS yields the lowest microgrid operational cost, and its low installation cost renders the total cost to be the lowest compared to other technologies, which makes it the optimal choice for this scenario.

It is noted from Table 3.5 that all BESS are selected to be installed in the first year, except for the Li-ion BESS which is deferred to the second year to reduce the NPV of its installation cost. The optimal power rating is 950 kW for all the technologies, while the energy capacity depends on the E/P ratio, efficiency, and the maximum DOD.

Table 3.5: Optimal installation decisions and related costs in Scenario 2

BESS Type	NaS	VRB	PbA	Li-ion
Year of Installation	Year 1	Year 1	Year 1	Year 2
P_{BESS}	950 kW	950 kW	950 kW	950 kW
E_{BESS}	5700 kWh	1300 kWh	1600 kWh	1150 kWh
INS	\$2,647,731	\$2,954,028	\$1,663,565	\$2,419,582
OM	\$58,957	\$475,520	\$367,125	\$1,008,962
$MGOC$	\$60,367,811	\$60,507,907	\$60,326,068	\$61,262,709
Total Costs	\$63,074,500	\$63,937,455	\$62,356,758	\$64,691,253

Adequate net generation is observed in Scenario 2, as shown in Figure 3.6. Because of the small energy capacity of VRB, PbA, and Li-ion BESS as compared to the NaS BESS, these technologies require recharging after the critical hours (8-11) to supply the reserve requirement at hour 20. The BCF of NaS BESS is less than other BESS technologies, it is 0.58% in year 10, while VRB, PbA, and Li-ion BESS are about 0.69%, 1.61%, and 1.09% in year 10, respectively.

It is noted that the microgrid operation is insecure, in terms of not having adequate reserves, before installing the BESS, as demonstrated in Figure 3.7. The reserve provided by DG units drops during the peak hours. Therefore, the BESS mainly supports the reserve provision of the microgrid. Since all BESS technologies suffer from energy losses when charging and discharging, it is preferred that these are only used as reserve provision, and less for meeting the energy needs, in this scenario, while DG units supply the demand. In such a case, the reserve provided by any type of BESS is more than that from DG units. The BRF of NaS, VRB, PbA, and Li-ion BESS are 70%, 67%, 69%, and 66% respectively, in year 10.

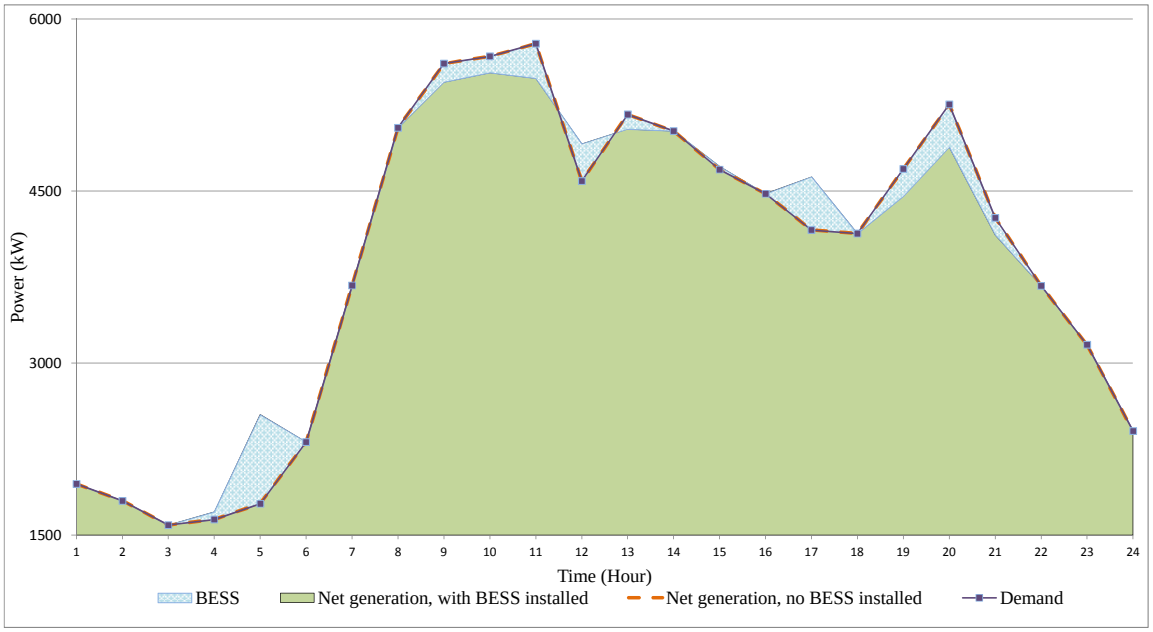

Figure 3.6: Supply and demand of year 10 in Scenario 2 (PbA BESS)

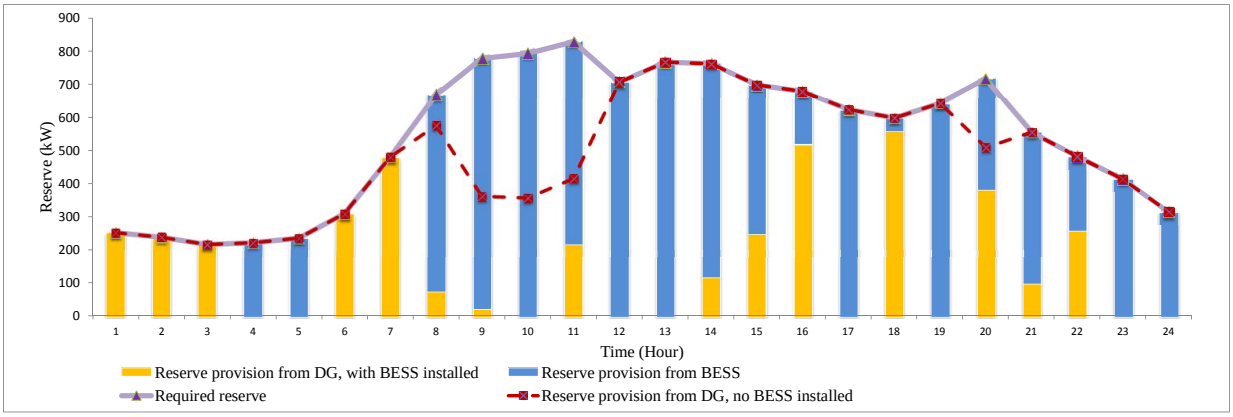

Figure 3.7: Reserve of year 10 in Scenario 2 (PbA BESS)

3.2.2.3 Scenario 3: Inadequate Microgrid Generation

This scenario considers a significant shortage in RES to the order of 90% over the plan horizon. Consequently, microgrid generation without BESS is lower than the demand, which also implies that the microgrid reserve is not sufficient. In this scenario, the BESS should be committed to discharge at peak hours to mitigate the mismatch between the microgrid generation and demand. At the same time, it should have the ability to meet the entire required reserve during these hours to ensure secure operation.

The microgrid operational cost before installing BESS is $90,978,640 (*not in table*), with total unserved energy of 315 kWh, occurring in years 8 to 10. Also, the required reserve is not met at some hours, starting from the first year itself. Therefore, BESS is required to be installed in the first year, as shown in Table 3.6.

Since more charging/discharging cycles are required, the microgrid operational cost is clearly affected by the efficiency of BESS technology. Since NaS and VRB BESS have lower efficiencies, the reduction in microgrid operational cost with these systems is less than that with PbA and Li-ion BESS. Although the efficiency of PbA and Li-ion BESS are similar, the selected size of PbA BESS is significantly larger than the Li-ion BESS because of its lower installation cost.

The energy capacity of NaS BESS is significantly large compared to the rest because of the E/P ratio constraint. As a result, the available capacity of the already committed DG units is used to charge the BESS during the first hours. The BESS then discharges all day without charging, until the late hours when the demand decreases again, while the smaller capacity of other BESS technologies requires their frequent charging. Figure 3.8 shows the supply-demand balance in case of PbA BESS. The BCF in year 10 for NaS, VRB, PbA, and Li-ion BESS are 2.28%, 2.75%, 3.81%, and 2.37%, respectively, which are higher than in the previous scenarios.

Table 3.6: Optimal installation decisions and related costs in Scenario 3

BESS Type	NaS	VRB	PbA	Li-ion
Year of Installation	Year 1	Year 1	Year 1	Year 1
P_{BESS}	1050 kW	1300 kW	1850 kW	1250 kW
E_{BESS}	6300 kWh	2550 kWh	3050 kWh	1950 kWh
INS	\$2,924,491	\$4,663,796	\$3,205,278	\$3,796,944
OM	\$68,482	\$657,055	\$714,644	\$2,347,525
$MGOC$	\$67,986,054	\$70,800,594	\$66,274,379	\$67,178,570
Total Costs	\$70,979,027	\$76,121,445	\$70,194,301	\$73,323,039

Figure 3.9 shows the reserve requirements in case of PbA BESS. The negative value of DG reserve before installing BESS means that even if the RES is increased by that value, RES generation will be used to supply the demand, while controllable DG units supply the demand at their maximum power ratings, implying that the microgrid operates without any reserve until further increase in generation.

The BESS dominates the share of reserve provided to the microgrid, the BRF for NaS, VRB, PbA, and Li-ion BESS are 73%, 78%, 65%, and 74%, respectively. It is noted that the BRF with PbA BESS in this scenario is lower than that in Scenario 2, although the required reserve has increased. This is because of two factors: first, the stored energy in the PbA BESS is mainly used for discharging in this scenario, as evident from its large BCF; hence, the SOC level is always low. Second, in order to compensate the loss of energy from BESS operational cycles, the MGO has to commit and schedule more DG units, thereby increasing the reserve capacity available from them.

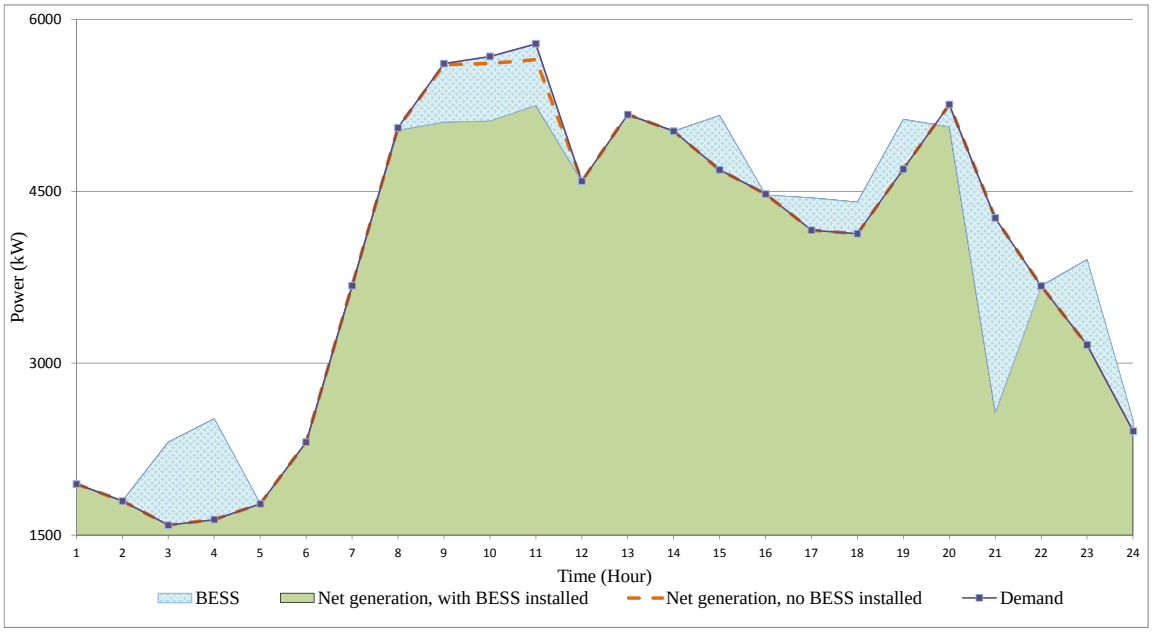

Figure 3.8: Supply and demand of year 10 in Scenario 3 (PbA BESS)

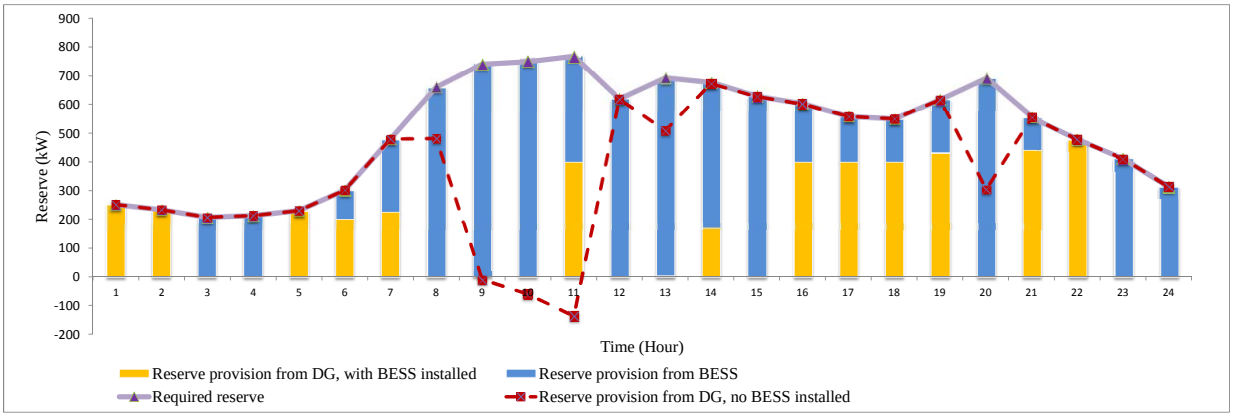

Figure 3.9: Reserve of year 10 in Scenario 3 (PbA BESS)

3.2.3 BESS Owned and Scheduled by Third-Party (Investor)

The ownership structure model in this case (discussed in Section 3.1.3.2) aims to determine the maximum amount of energy that can be exchanged with the microgrid for a certain discharge price (¢/kWh). The BESS size is determined from an optimistic viewpoint to capture the maximum profit for an investor. Although in reality, the BESS may not discharge this amount of energy to the microgrid, this study seeks to find the minimum acceptable discharge price for the investor that recovers the installation and operating cost of the BESS.

The model considers the RES profile of the third scenario, where RES availability is low and therefore in the most favourable condition for the investor. The revenue is accrued from supplying energy to the microgrid and from providing reserve, while the installation and O&M cost is paid by the third party. Since the system is isolated, hourly market prices are not applicable, and it is assumed that the charge price is fixed at 1 ¢/kWh, while the discharge price is varied in the range 2.5 ¢/kWh and 37.5 ¢/kWh. The price of BESS reserve is assumed to be 0.6 ¢/kW [5]. The rate of return for the investor is considered to be 14%.

As shown in Figure 3.10, different BESS technologies are examined to investigate the profit for the investor over a range of discharge prices. It is shown that PbA BESS is the best choice for the third party since the minimum acceptable discharge price that generates profit is 12.5 ¢/kWh, which is the lowest across the BESS technologies. The PbA BESS is followed by NaS, Li-ion, and VRB BESS with a minimum acceptable discharge price of 15 ¢/kWh, 20 ¢/kWh, and 25 ¢/kWh, respectively. The optimal power and energy size of BESS and the installation year at the minimum discharge prices that generates profit, are presented in Table 3.7.

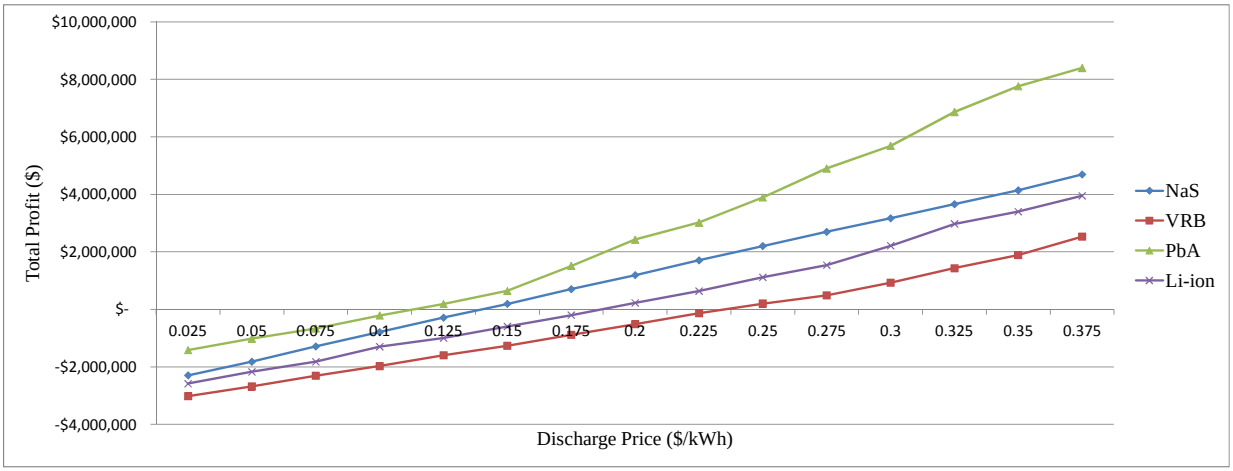

Figure 3.10: Discharge price impact on total profit

Table 3.7: Optimal installation decisions at the minimum profit point (investor's perspective)

BESS Type	NaS	VRB	PbA	Li-ion
Year of Installation	Year 1	Year 1	Year 1	Year 1
P_{BESS}	1050 kW	1050 kW	1050 kW	1100 kW
E_{BESS}	6300 kWh	2050 kWh	2550 kWh	1500 kWh
θ_{dch}	15 ¢/kWh	25 ¢/kWh	12.5 ¢/kWh	20 ¢/kWh
DCH REV	$2,975,273	$3,870,797	$2,233,353	$3,304,285
Reserve REV	$317,816	$239,963	$245,932	$203,715
CH Cost	$262,058	$224,752	$197,970	$183,063
INS	$2,770,570	$3,564,605	$1,928,596	$2,996,842
OM	$68,627	$120,216	$167,469	$100,085
Total Profit	$191,834	$201,186	$185,249	$228,010

3.3 Summary

A new mathematical model was proposed in this chapter for determining the optimal year of installation and sizing of BESS in isolated microgrids. The model takes into consideration the optimal BESS operation for any microgrid condition. Two BESS ownership structures are considered.

In the first structure, the BESS is owned and scheduled by the MGO. Three scenarios of RES profiles are considered to examine the BESS optimal installation and operation. When BESS is not assigned for a certain application, it is mainly used to enhance total microgrid operation via load leveling and helping the DG units to meet the required reserves. However, when the BESS is assigned to support the microgrid operation for a certain application during certain hours, the proposed model coordinates between satisfying the microgrid requirements and enhancing the total microgrid operation. The size and year of installation are determined based on the optimal BESS operation which is affected by the inherent characteristics of BESS technology.

The second ownership structure studies the optimal installation decisions when the BESS is installed by a third party and scheduled from its perspective of profit maximization. The maximum size of BESS that the investor is willing to install for a certain discharge price is determined for various technologies. Also, a minimum acceptable discharge price for each BESS technology is determined at which the installation would make profit for the investor.

Since the optimal BESS installation decisions depends mainly on the specific microgrid operation considered, the optimal BESS size and corresponding operation may not be optimal for other scenarios. Therefore, a stochastic model should be developed to consider wider range of possible microgrid operation scenarios as will be discussed in next chapter.

Chapter 4

A Decomposition Based Approach to Stochastic Optimal Planning of BESS

The uncertain nature of RES and demand in microgrids imposes more challenges in energy storage planning. The selection of the optimal type of BESS technology and the optimal size will be investigated in this chapter considering the uncertain behavior of the microgrid demand, wind and PV profiles. Unlike the deterministic model, the size of the problem is large, and thus, it cannot be solved in a single stage. Therefore, a decomposition based approach is proposed that determines the planning decisions in two stages. In the first stage, the optimal BESS power and energy ratings are determined, while the second stage identifies the optimal year of installation for the determined size. Numerical results and a comparison between the four types of BESS technologies is presented.

4.1 Mathematical Model for Stochastic Optimal Planning of BESS

The proposed planning model seeks to determine the optimal BESS power and energy ratings as well as the installation year considering uncertainty in demand, and in the output from RES.

4.1.1 Objective Function

The objective is to minimize the NPV of the total costs including the BESS installation cost, O&M cost, and microgrid operational cost.

$$J_3 = INS + OM + MGOC \tag{4.1}$$

Two variable cost components, proportional to the installed power and energy ratings of the BESS, Cp^v and Ce^v respectively, are considered in the installation cost, in addition to the fixed cost (C^f) which does not depend on the size. The NPV of the BESS installation cost is formulated as follows:

$$INS = \sum_{y=1}^{Y_T} \Big[\frac{1}{(1+\alpha)^y} Z_y (Cp^v P_{BESS} + Ce^v E_{BESS} + C^f) \Big] \tag{4.2}$$

In the O&M cost, an annual fixed cost (OMC^f) and the replacement cost (RC) are considered proportional to the BESS size. The O&M variable cost (OMC^v) depends on the energy discharged

by the BESS. The NPV of the total expected operational cost of the BESS is given as follows:

$$\begin{aligned} OM = & \sum_{y=1}^{Y_T} \Big[\frac{1}{(1+\alpha)^y} \, OMC^f \, P_{BESS} \, Zc_y \Big] \\ & + 365 \times \sum_{s=1}^{S} \rho_s \sum_{y=1}^{Y_T} \sum_{h=1}^{H} \Big[\frac{1}{(1+\alpha)^y} \, OMC^v \, \big(\frac{Eff_{ch}}{1 - Eff_{ch} Eff_{dch}} \big) (- PB_{s,y,h}) \Big] \\ & + \sum_{y=RY}^{Y_T} \Big[\Big(\frac{1}{(1+\alpha)^y} + \frac{1}{(1+\alpha)^{y+RY}} + ... \Big) \, RC \, P_{BESS} \, Z_{y-RY+1} \Big] \end{aligned} \tag{4.3}$$

The binary variable Zc_y in (4.3), denoting the presence of BESS in the system from year y onwards, is determined from the binary variable Z_y which denotes the BESS installation decision at year y. Accordingly, Zc_y is given as:

$$Zc_y = \sum_{n=1}^{y} Z_n \qquad \forall y \tag{4.4}$$

The NPV of the expected operational cost of the microgrid is given as follows:

$$\begin{aligned} MGOC = 365 \times \sum_{s=1}^{S} \rho_s \sum_{y=1}^{Y_T} \sum_{h=1}^{H} \sum_{i=1}^{I} \Big[\frac{1}{(1+\alpha)^y} \Big[& (1+\beta)^{y-1} F_i(P_{s,y,h,i}) W_{s,y,h,i} \\ & + SU_i U_{s,y,h,i} + SD_i V_{s,y,h,i} \Big] \Big] \end{aligned} \tag{4.5}$$

where $F_i(\cdot)$ is the operational cost function of a DG. It is to be noted that some of the variables in (4.3) and (4.5) have an additional index denoting the scenario. This is to capture the uncertainty in various parameters which are modeled in this work using probability distribution functions. Each uncertain scenario has an associated probability ρ_s, in (4.3) and (4.5) and the optimal decisions are now determined for every scenario, year, and hour while minimizing the *expected* costs.

4.1.2 Model Constraints

As mentioned earlier, the variables in each of the constraints discussed below are now specified for a scenario of uncertainty, in addition to its other indices.

Demand-Supply Balance: This ensures sufficient generation from DG units and RES to meet the microgrid demand at an hour.

$$\sum_{i=1}^{I} P_{s,y,h,i} + PB_{s,y,h} + PV_{s,y,h} + Pw_{s,y,h} = Pd_{s,y,h} \qquad \forall s, \forall y, \forall h \tag{4.6}$$

Dispatchable DG units Constraints: These are similar to the ones presented in Chapter 2, and given by constraints (2.13) to (2.22) with considering the indices s and y.

Microgrid Reserve Requirements: The MGO ensures a minimum reserve level of 10% of the demand plus factors accounting for uncertainty in demand and RES forecasting errors [25], [55]. The reserve constraint is modeled as follows:

$$RTH_{s,y,h} + RB_{s,y,h} \geq (0.1 + \delta_D)Pd_{s,y,h} + \delta_{PV}PV_{s,y,h} + \delta_W Pw_{s,y,h} \qquad \forall s, \forall y, \forall h \tag{4.7}$$

$$RTH_{s,y,h} \leq \sum_{i=1}^{I} (\overline{P_i} W_{s,y,h,i} - P_{s,y,h,i}) \qquad \forall s, \forall y, \forall h \tag{4.8}$$

$$RB_{s,y,h} \leq -PB_{s,y,h} + \min\left\{[SOC_{s,y,h} - Zc_y\, E_{BESS}(1 - \overline{DOD})]Eff_{dch}, P_{BESS}\right\} \qquad \forall s, \forall y, \forall h \tag{4.9}$$

The above set of equations (4.7)-(4.9) are quite similar to those in Chapter 3, equations (3.21)-(3.23) excepts for the presence of scenarios of uncertainty in the present ones.

BESS Operational Constraints:

The relationship between the charging and discharging power of the BESS and its SOC can be described as follows:

$$\frac{PB_{s,y,h}}{Eff_{dch}} Zdch_{s,y,h} + PB_{s,y,h} Eff_{ch} Zch_{s,y,h} = SOC_{s,y,h} - SOC_{s,y,h+1} \qquad \forall s, \forall y, \forall h; h \neq 24 \tag{4.10}$$

The initial and final SOC of the BESS are assumed to be 50% of the installed energy capacity. The initial SOC is formulated as:

$$SOC_{s,y,h} = 0.5\ E_{BESS}\ Zc_y \qquad \forall s, \forall y, h = 1 \tag{4.11}$$

The final status of SOC is implemented by replacing $SOC_{s,y,h+1}$ in (4.10) to the desired level of SOC (i.e. 50% of the energy capacity), as follows:

$$\frac{PB_{s,y,h}}{Eff_{dch}} Zdch_{s,y,h} + PB_{s,y,h} Eff_{ch} Zch_{s,y,h} = SOC_{s,y,h} - (0.5\ E_{BESS}\ Zc_y) \qquad \forall s, \forall y, h = 24 \tag{4.12}$$

To prevent simultaneous charging and discharging, the following constraint is considered.

$$Zch_{s,y,h} + Zdch_{s,y,h} \leq Zc_y \qquad \forall s, \forall y, \forall h \tag{4.13}$$

The BESS power and SOC limits are formulated as follows:

$$(1 - \overline{DOD}) E_{BESS}\ Zc_y \leq SOC_{s,y,h} \leq E_{BESS}\ Zc_y \qquad \forall s, \forall y, \forall h \tag{4.14}$$

$$-P_{BESS}\ Zc_y \leq PB_{s,y,h} \leq P_{BESS}\ Zc_y \qquad \forall s, \forall y, \forall h \tag{4.15}$$

BESS Sizing Constraints:

This constraint ensures that Z_y is only activated once during the planning horizon, denoting the year of installation, as follows:

$$\sum_{y=1}^{Y_T} Z_y \leq 1 \tag{4.16}$$

To activate Z_y when BESS is installed, the following constraint is considered.

$$P_{BESS} \leq M \sum_{y=1}^{Y_T} Z_y \tag{4.17}$$

The energy capacity of the BESS for a certain power rating, is determined based on its energy to power ratio, as follows:

$$\underline{EPR}\, P_{BESS} \leq E_{BESS} \leq \overline{EPR}\, P_{BESS} \tag{4.18}$$

Budget Constraint:

The NPV of the installation cost should not exceed the NPV of the allocated budget for the year.

$$INS \leq B_0 \tag{4.19}$$

The planning problem formulated in (4.1)-(4.19) is a stochastic mixed integer non-linear programming (MINLP) model, and has been referred to as Optimal Power and Energy Sizing (OPES) model in the subsequent sections of this chapter.

4.2 Proposed Decomposition Approach for Solving the Stochastic BESS Planning Problem

The MINLP model presented in Section 4.1 is computationally very challenging, particularly because of the presence of large number of probabilistic scenarios. Therefore, the problem is decomposed into two stages. Stage-I determines the BESS power and energy ratings based on the terminal year. Then, the OPES model is solved in Stage-II with fixed P_{BESS} and E_{BESS} for the entire planning period to determine the BESS year of installation.

It is to be noted that fixing the binary variable (Z_y) at unity in Stage-I and the BESS ratings (P_{BESS} and E_{BESS}) in Stage-II allows solving the problem as a MILP model. Equations (4.10) and (4.12) are linearized using the same approach presented in (3.36)-(3.41) but considering the scenario index in the variables.

The proposed decomposition approach is solved iteratively, as shown in Figure 4.1. In Stage-I, the OPES model determines the optimal BESS size assuming that the BESS is installed at the terminal year. Consequently, the installation cost is discounted to the terminal year which allows installing large power and energy ratings of BESS. Although the budget is adequate for a large BESS, the size is optimized considering the BESS effect on microgrid operations.

Stage-II solves the OPES model considering the entire planning period and fixing the BESS size determined at the terminal year. The BESS can either be installed at an earlier year of the planning horizon to incur higher the benefits or can be deferred to reduce the NPV of the installation cost. The OPES model in Stage-II seeks the optimal year of installation that yields minimum cost with maximum benefit. If the budget is not sufficient for installation of BESS for the given size, the OPES model defers the year of installation to reduce the NPV and hence meet the budget constraint. Furthermore, if for any of the considered scenarios, the operational

constraints are not satisfied, then the selected BESS size is not feasible.

In such a case, the BESS size is reduced by tightening the budget constraint to allow installing the BESS at an earlier year. This is performed iteratively by limiting the budget based on the installation cost of the BESS size determined in the terminal year.

Infeasible solution in the first iteration of the OPES model implies that the allocated budget is less than the installation cost required for the minimum BESS size in the terminal year. In any other iteration, an infeasible solution is obtained when the installation cost cannot be reduced further, which means the BESS size required for the terminal year is at its minimum level. Therefore, if the installation cost of the minimum BESS size required for the terminal year does not meet the budget constraint at an earlier year, where a BESS is also required, then the problem is infeasible because of violating the microgrid operation requirements.

4.3 Results and Analysis

4.3.1 Microgrid Test System

The proposed decomposition based approach is applied to the same microgrid test system used in Chapter 3. In order to account for the uncertainty, several probabilistic states of demand, wind and PV generation are considered at each hour. Each of these uncertain parameters are modeled considering a normal probability distribution function, with five uncertain states for the demand and wind generation, and three uncertain states for PV generation [58]. Therefore, for each hour, there are 75 scenarios with a probability associated with it. The deviation level in [58] is slightly increased here to account for a wider range of uncertainties, as shown in Table 4.1. Figure 4.2, Figure 4.3, and Figure 4.4 shows the deviation of the states from the forecasted profile, for demand, wind and PV generation, respectively.

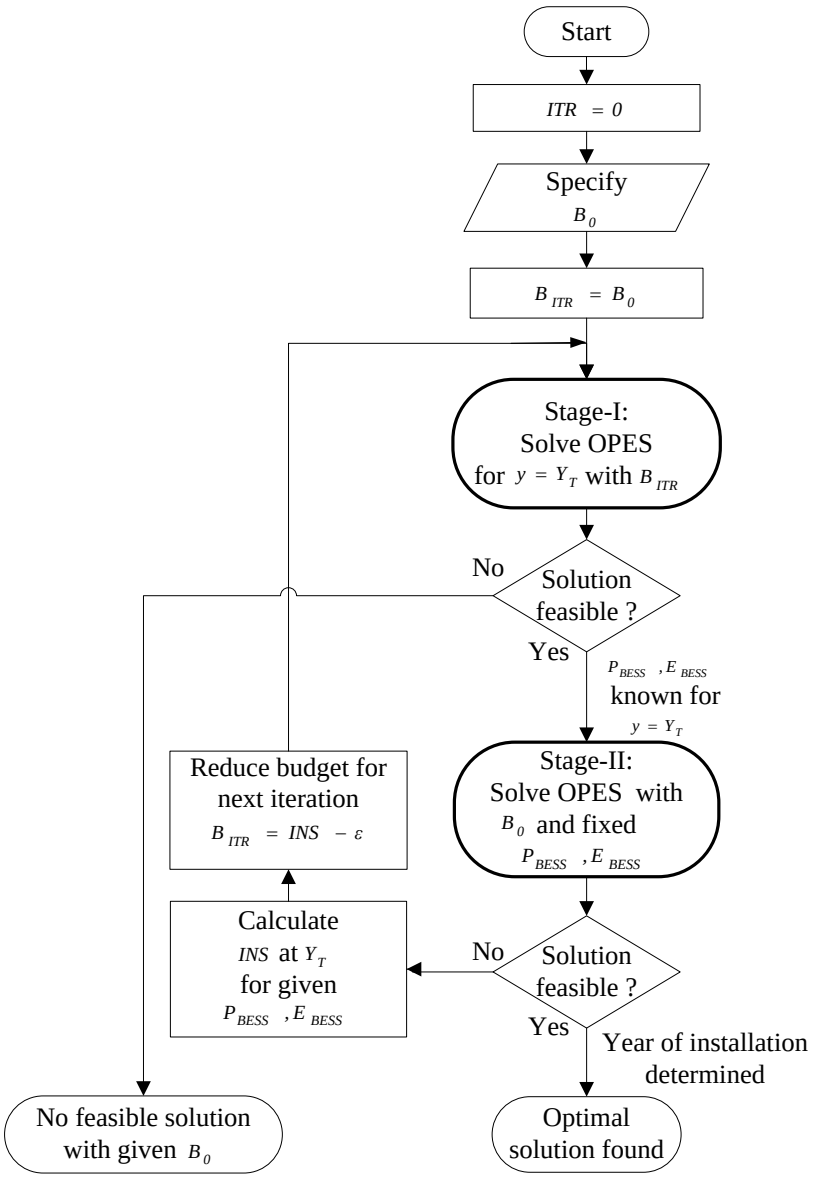

Figure 4.1: Schematic for the decomposition based stochastic optimal planning of BESS

Table 4.1: Probability distribution functions of the uncertain states

	Demand	Probability	Wind	Probability	PV	Probability
High state	+6%	0.05	+6%	0.1		
Mid-high state	+3%	0.15	+3%	0.15	+4%	0.15
Forecasted value	Nominal	0.6	Nominal	0.5	Nominal	0.7
Mid-low state	-3%	0.15	-3%	0.15	-4%	0.15
Low state	-6%	0.05	-6%	0.1		

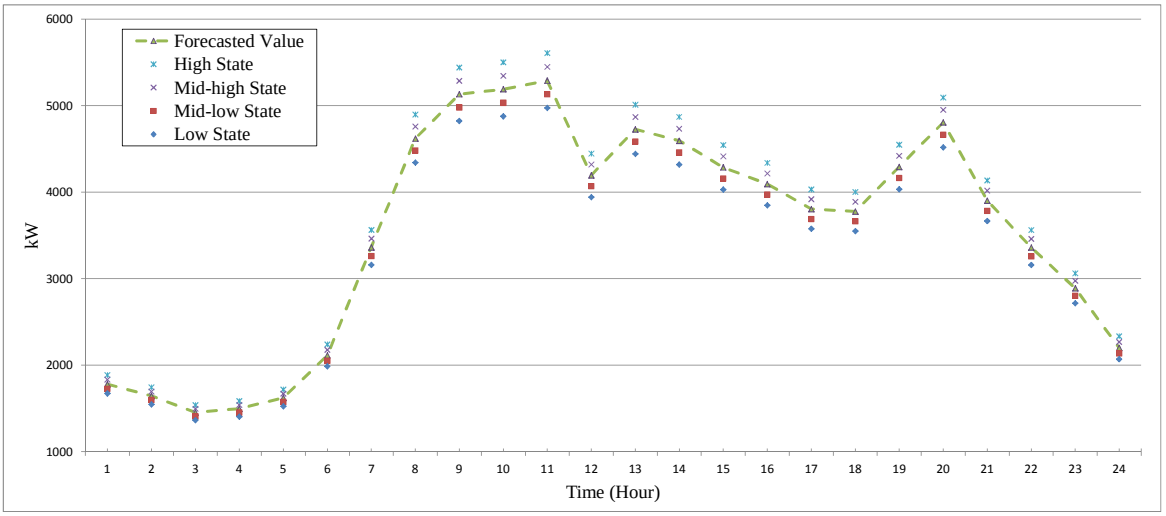

Figure 4.2: Hourly demand states for a typical day of the first planning year

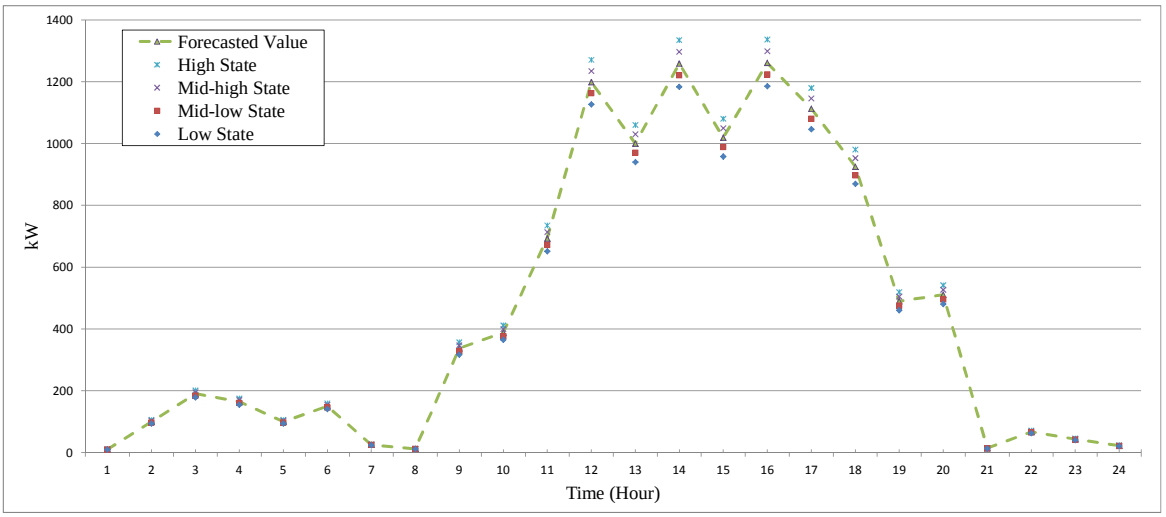

Figure 4.3: Hourly wind generation states for a typical day of the first planning year

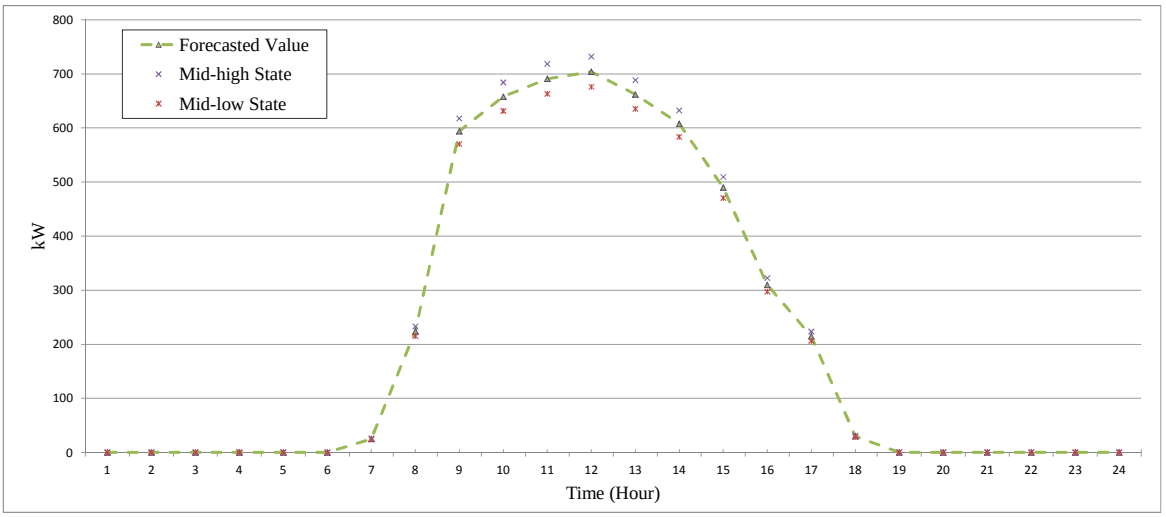

Figure 4.4: Hourly PV generation states for a typical day of the first planning year

4.3.2 Case Studies

Two distinct cases of BESS planning are considered as follows:

(a) *Case-1: No budget limit* - The available budget for BESS installation is sufficient to install a large size of BESS at any year. Stage-I determines the optimal size for BESS, both P_{BESS} and E_{BESS}, while Stage-II determines the optimal year of installation considering the entire planning horizon.

(b) *Case-2: Imposition of budget limit* - When considering a limited budget, the BESS size and installation year may not be obtained in a single iteration as in Case 1. Therefore, several iterations may be required to arrive at an optimal solution. In this case, a budget limit of $1.3 million is considered.

4.3.2.1 NaS BESS

The optimal decisions are presented in Table 4.2. In Case 1, the optimal power rating (P_{BESS}) obtained in Stage-I is 550 kW, and considering the range of the E/P ratios available for NaS BESS, the installed E_{BESS} cannot be less than 3,300 kWh. In Stage-II, NaS BESS is recommended to be installed in the first year. This is because of the large energy capacity and power rating, which necessitates installation in the first year so as to accrue the microgrid benefit. Furthermore, NaS BESS does not require replacement within the 10-year plan horizon, which reflects on its low O&M cost and allows earlier installation. The total expected cost before installing BESS is $59,201,654 (*not in table*) which is reduced by 5.01% after installing the NaS BESS.

Stage-I decisions in Case 2 are identical to that in Case 1 to allow installing the largest possible size. Contrary, Stage-II shows different results in Case 2; the installation is deferred to

the fourth year in order to meet the budget limit. Figure 4.5 demonstrates the impact of limiting the budget on the planning decisions in Stage-II. The line in the figure represents the NPV of the installation cost for the determined BESS size from Stage-I. The optimal year of installation in Case 1 is selected to be in the first year, while when imposing the budget limit, the selected size of BESS can only be installed after the third year to meet the budget constraint. This decision leads to a feasible solution of OPES in Stage-II which is considered as the optimal solution for Case 2. The reduction of total expected cost in Case 2 is about 3.72% from the case of no BESS installed. It can be noted that the total cost in Case 1 is less than that in Case 2 by $764,613 because of the smaller BESS size as well as the later installation year in Case 2.

Table 4.2: NaS BESS planning decisions

		Case 1	Case 2
		Iteration 1	Iteration 1
STAGE-I	P_{BESS}	550 kW	550 kW
	E_{BESS}	3300 kWh	3300 kWh
	INS at Y_T	$770,731	$770,731
	OM at Y_T	$2,351	$2,351
	$MGOC$ at Y_T	$4,705,860	$4,705,860
	Total costs at Y_T	$5,478,941	$5,478,941
	Model status	integer optimal	integer optimal
	Solving time (sec)	693	693
STAGE-II	Year of installation	1	4
	INS	$1,540,694	$1,223,053
	OM	$34,101	$20,988
	$MGOC$	$54,659,587	$55,754,954
	Total costs	$56,234,382	$56,998,995
	Model status	integer optimal	integer optimal
	Solving time (sec)	43,259	43,270

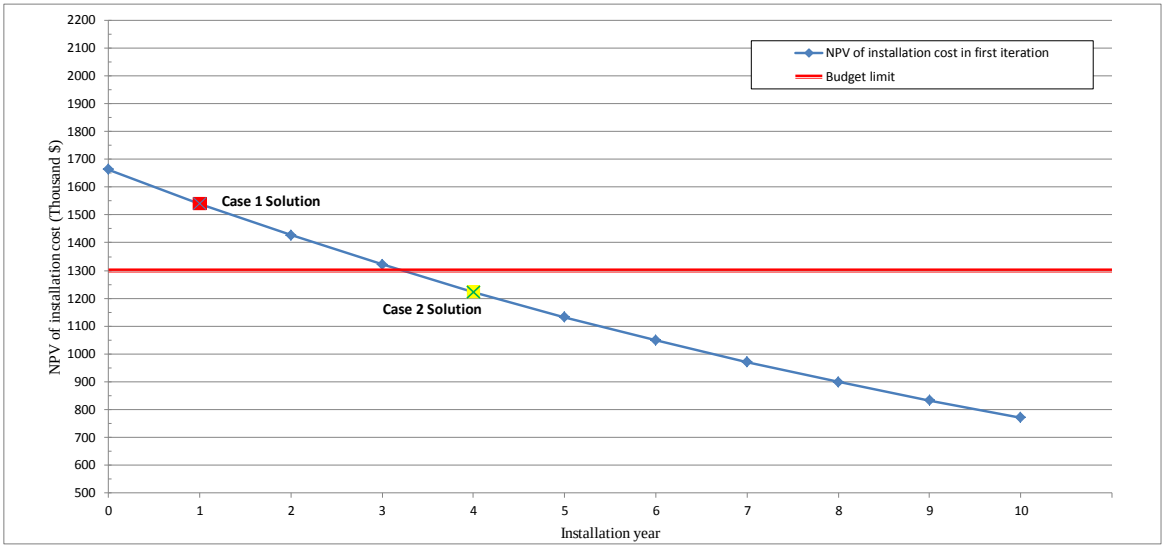

Figure 4.5: The impact of imposing budget limit on NaS BESS installation

4.3.2.2 VRB BESS

A single iteration is required to obtain the optimal solution for VRB BESS in Case 1, while Case 2 requires two iterations to arrive at a feasible OPES solution, as shown in Table 4.3.

In Case 1, the determined ratings for VRB BESS are 550 kW and 800 kWh. The second year is the optimal installation year for VRB BESS. The total expected cost in Case 1 is $56,902,473.

In Case 2, the size obtained from Stage-I in the first iteration is similar to the selected in Case 1. However, the selected BESS size in the first iteration can only be installed after year 4 in Case 2 to meet the budget limit, as shown in Figure 4.6. The OPES model in Stage-II does not yield a feasible solution, and hence a second iteration is required to revise the determined size in Stage-I. The new iteration budget (B_{ITR}) in Stage-I is reduced to be less than $878,748. The revised BESS size in the second iteration is reduced by 50 kW and 50 kWh. The OPES model in Stage-II reveals that the optimal installation year for VRB BESS is year 4.

It is noted that the BESS O&M cost is stepped down significantly in Case 2 since the replacement cost in Case 1, which is about $251,783, is not applicable because of the late installation year. However, the microgrid operational cost in Case 2 is increased by $1,410,751 because of the smaller BESS size and the deferred installation from year 2 to year 4. As a result, the total cost in Case 2 is increased by $850,994 than that in Case 1. The total expected cost before installing VRB BESS is reduced by 3.88% and 2.45% in Case 1 and Case 2, respectively.

Table 4.3: VRB BESS planning decisions

		Case 1	Case 2	
		Iteration 1	Iteration 1	Iteration 2
STAGE-I	P_{BESS}	550 kW	550 kW	500 kW
	E_{BESS}	800 kWh	800 kWh	750 kWh
	INS at Y_T	$878,748	$878,748	$808,967
	OM at Y_T	$4,293	$4,293	$3,902
	$MGOC$ at Y_T	$4,717,470	$4,717,470	$5,317,853
	Total costs at Y_T	$5,600,511	$5,600,511	$6,130,722
	Model status	integer optimal	integer optimal	integer optimal
	Solving time (sec)	664	664	24,131
STAGE-II	Year of installation	2	-	4
	INS	$1,626,500	-	$1,283,730
	OM	$251,783	-	$34,797
	$MGOC$	$55,024,190	-	$56,434,941
	Total costs	$56,902,473	-	$57,753,467
	Model status	integer optimal	integer infeasible	integer optimal
	Solving time (sec)	3,935	4	17,253

4.3.2.3 PbA BESS

In the two considered cases, a single iteration is required to obtain the optimal solution for PbA BESS, as shown in Table 4.4. In Case 1, the optimal ratings for PbA BESS are 900 kW and 1200 kWh, while the optimal year of installation is year 2. Figure 4.7 shows that the BESS of the determined size meets the budget limit if it is installed in year 3, which is found to be feasible OPES solution.

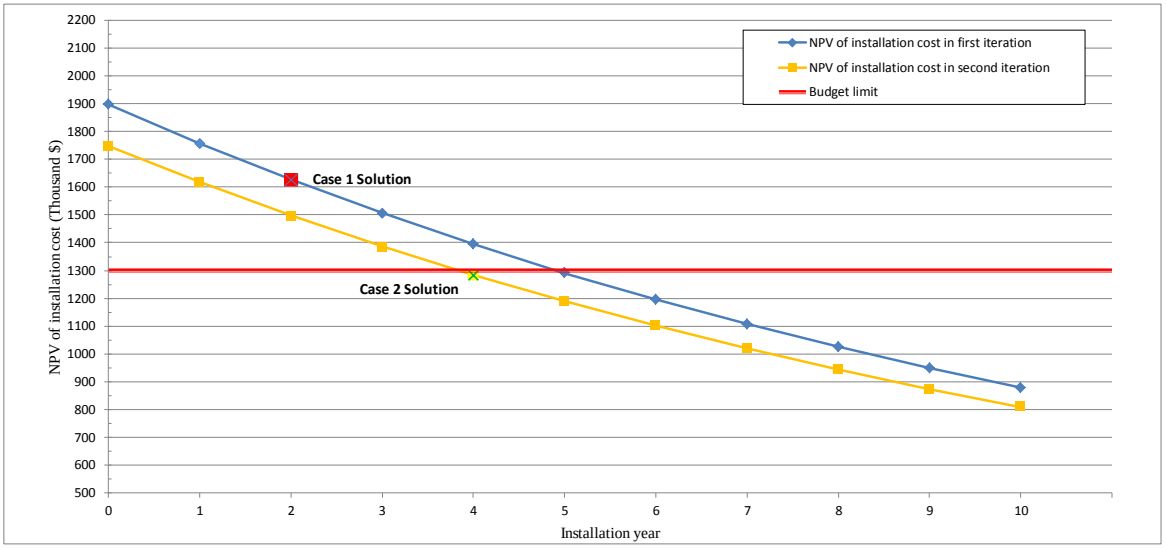

Figure 4.6: The impact of imposing budget limit on VRB BESS installation

The PbA BESS has the lowest total expected cost across the BESS technologies in both cases. The impact of imposing the budget is not significant compared to the results obtained for other BESS technologies. The total expected cost in Case 1 and Case 2 are \$56,183,506 and \$56,518,472, respectively, and the reduction in total expected cost from the case of no BESS are 5.1% and 4.53%, respectively.

4.3.2.4 Li-ion BESS

The optimal decisions for Li-ion BESS are shown in Table 4.5. In Case 1, the optimal Li-ion BESS ratings are 650 kW and 850 kWh. The optimal installation year is 2. Four iterations are required to obtain the optimal solution in Case 2. In the first iteration, the determined BESS size from Stage-I cannot be installed earlier than year 6, as shown in Figure 4.8, which yields an infeasible solution and requires revising the size. In the second iteration, the iteration budget limit B_{ITR} in Stage-I is determined to be less than \$923,700. Therefore, the size is reduced in the

Table 4.4: PbA BESS planning decisions

		Case 1	Case 2
		Iteration 1	Iteration 1
STAGE-I	P_{BESS}	900 kW	900 kW
	E_{BESS}	1200 kWh	1200 kWh
	INS at Y_T	$748,660	$748,660
	OM at Y_T	$11,382	$11,382
	$MGOC$ at Y_T	$4,635,201	$4,635,201
	Total costs at Y_T	$5,395,243	$5,395,243
	Model status	integer optimal	integer optimal
	Solving time (sec)	1,415	1,415
STAGE-II	Year of installation	2	3
	INS	$1,385,717	$1,283,071
	OM	$310,373	$276,960
	$MGOC$	$54,487,417	$54,958,441
	Total costs	$56,183,506	$56,518,472
	Model status	integer optimal	integer optimal
	Solving time (sec)	3,960	3,277

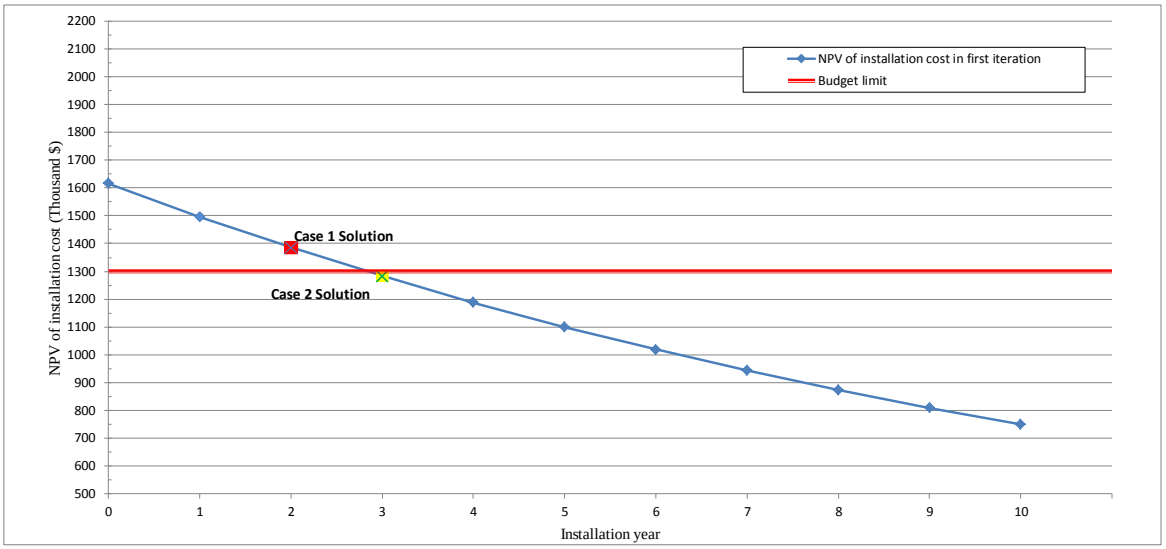

Figure 4.7: The impact of imposing budget limit on PbA BESS installation

second iteration and then the third iteration since a feasible solution cannot be obtained from the OPES model in Stage-II. The final revised Li-ion BESS ratings in iteration four are 550 kW and 750 kWh. Stage-II reveals that year 4 is the optimal year of installation for Li-ion BESS.

Although the installation of Li-ion BESS is deferred from year 2 to year 4, same as VRB BESS, the O&M of Li-ion BESS does not decrease significantly since the replacement cost is assumed to be every five years of operation, which is applied in Case 1 and Case 2. The difference in the total expected cost between the two cases is $344,619. The reduction in total expected cost after installing the Li-ion BESS is about 3.42% and 2.84% for Case 1 and Case 2, respectively.

Table 4.5: Li-ion BESS planning decisions

		Case 1	Case 2			
		Iteration 1	Iteration 1	Iteration 2	Iteration 3	Iteration 4
STAGE-I	P_{BESS}	650 kW	650 kW	650 kW	600 kW	550 kW
	E_{BESS}	850 kWh	850 kWh	800 kWh	750 kWh	750 kWh
	INS at Y_T	$923,700	$923,700	$902,834	$838,913	$795,859
	OM at Y_T	$4,062	$4,062	$4,058	$3,742	$3,430
	$MGOC$ at Y_T	$4,691,479	$4,691,479	$4,697,747	$4,761,881	$4,843,207
	Total costs at Y_T	$5,619,242	$5,619,242	$5,604,639	$5,604,536	$ 5,642,496
	Model status	integer optimal	integer optimal	integer optimal	integer optimal	integer optimal
	Solving time (sec)	2,463	2,463	387	550	1,114
STAGE-II	Year of installation	2	-	-	-	4
	INS	$1,709,705	-	-	-	$1,262,928
	OM	$689,764	-	-	-	$494,210
	$MGOC$	$54,775,655	-	-	-	$55,762,605
	Total costs	$57,175,124	-	-	-	$57,519,743
	Model status	integer optimal	integer infeasible	integer infeasible	integer infeasible	integer optimal
	Solving time (sec)	3,306	4	4	3	2,173

4.4 Summary

In this chapter, a decomposition-based approach is proposed to determine the expected year of installation and sizing of BESS in isolated microgrids. The proposed stochastic model considers

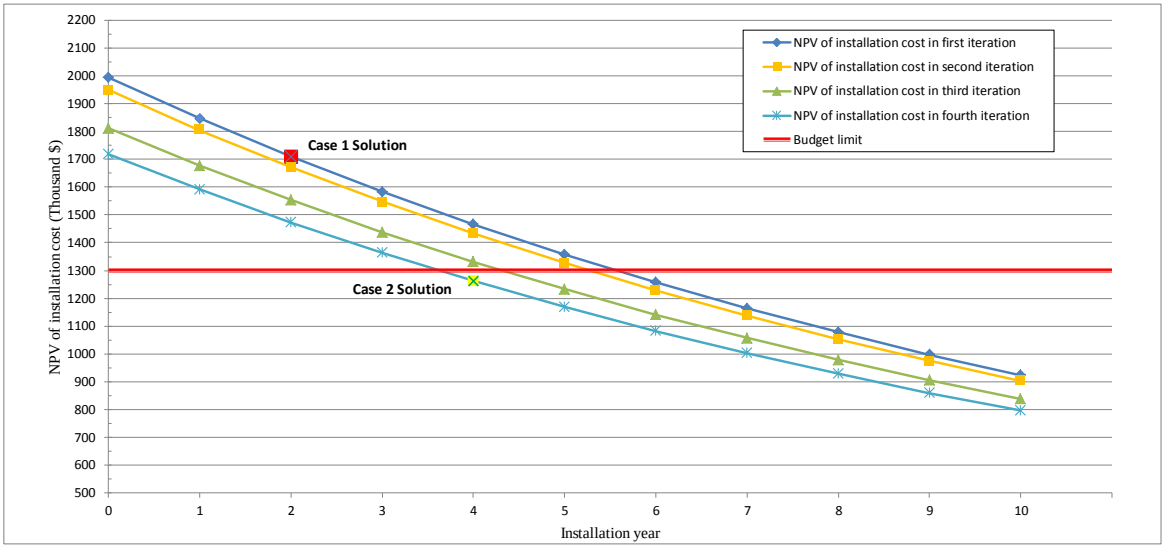

Figure 4.8: The impact of imposing budget limit on Li-ion BESS installation

the uncertainty of microgrid variables: solar radiation, wind speed, and load, using different probabilistic scenarios. The optimal BESS plan decisions and operations are determined to achieve maximum reduction in microgrid operating cost from the BESS applications, load levelling and reserve, at the least installation cost.

Since the stochastic problem is large, the proposed decomposition approach determines the optimal decisions in two stages. The budget limit affects the solution and may not yields feasible solution. Therefore, the approach considers relaxing the budget constraint to ensure the optimal decision, then the budget constraint is imposed in the model in steps until arriving at a feasible solution that meets the budget limit.

Two case studies are conducted to examine the impact of the available budget on the four BESS technologies. Results show the feasibility and effectiveness of the proposed approach to determine the BESS power and energy size along with the installation year.

Chapter 5

Conclusions

5.1 Summary

The optimal planning decisions of BESS installation are addressed in this thesis for isolated microgrids. The proposed optimization models determine the BESS power and energy size and the year of installation over the planning horizon based on the optimal scheduling of the BESS and microgrid resources. Some common BESS technologies are examined, considering their inherent characteristics to compare between the different options. In Chapter 1, the motivations and objectives of the research are presented. This is followed by a review of literature addressing the energy storage systems sizing problem. In Chapter 2, an overview of the microgrid concept, the technical issues in grid-connected and isolated microgrids and real examples of microgrids are discussed. Then, energy storage technologies and their characteristics, and the main properties of energy storage systems are presented. This chapter also presents the generic UC model formulation. In Chapter 3, the novel optimization model to determine the BESS size and installation year is proposed considering different scenarios of

RES profiles and BESS ownership structures. In Chapter 4, the uncertainty of microgrid demand, PV, and wind generation are considered. A novel decomposition based approach is proposed to solve the stochastic planning problem and hence obtain the expected BESS size and installation year in two stages. The approach is solved iteratively to ensure utilizing the allocated budget.

5.2 Contributions

The main contributions of this thesis are as follows:

- A new optimization model is proposed to determine the optimal power and energy ratings and installation year of BESS for isolated microgrids considering four different BESS technologies. The optimal decisions minimize the NPV of total costs taking into consideration the optimal BESS operation. The BESS is modeled to enhance the microgrid operation by levelling the load and also providing the reserve to the microgrid in conjunction with the spinning reserve from DG units.

- The microgrid reserve is modeled to allow the BESS to support the DG units in providing the required reserves. Three modes of operation of the BESS, charging, discharging, and standby, are considered when providing the reserve.

- Several scenarios considering different BESS ownership structures are examined. The objective functions are modeled to include the corresponding BESS energy costs in addition to the BESS installation cost or the microgrid operational cost.

- A new approach to determine the minimum acceptable discharge price for third-party investors in BESS is proposed, and the optimal sizing is determined considering investor

profit maximization as the objective.

- A novel decomposition-based approach is proposed to solve the stochastic planning problem for BESS and hence determine the expected size and installation year for BESS under uncertainty. The proposed approach is solved in two stages to ensure the convergence of the stochastic optimization problem. The power and energy ratings are determined in the first stage, while the installation year is determined in the second stage. The approach ensures utilizing the allocated budget effectively by performing several iterations.

5.3 Future Work

- The model can be modified to include the seasonal impact of demand, PV, and wind profiles. However, the computation time will increase in proportion with the resolution of the considered profiles.
- Sizing BESS in smart microgrids considering demand response and plug-in electric vehicles is a potential extension of this work.
- Consideration of the dissipation factor in modeling BESS life cycle and considering the standby loss.
- The stochastic model can be improved by considering a larger range of uncertainties, and also compare with Monte Carlo Simulation.

References

[1] R. H. Lasseter, "Microgrids," in *IEEE Power Eng. Soc. Winter Meeting*, vol. 1, 2002, pp. 305–308.

[2] Q. Jiang, M. Xue, and G. Geng, "Energy management of microgrid in grid-connected and stand-alone modes," *IEEE Trans. Power Syst.*, vol. 28, no. 3, pp. 3380–3389, Aug. 2013.

[3] M. Arriaga, C. A. Canizares, and M. Kazerani, "Northern lights: Access to electricity in Canada's northern and remote communities," *IEEE Power and Energy Magazine*, vol. 12, no. 4, pp. 50–59, Jul. 2014.

[4] V. Rious and Y. Perez, "What type(s) of support schemes for storage in island power systems?" Robert Schuman Centre for Advanced Studies, RSCAS 2012/70, 2012.

[5] J. Eyer and G. Corey, "Energy storage for the electricity grid: Benefits and market potential assessment guide," Sandia National Laboratories, Albuquerque, NM and Livermore, CA, SAND2010-0815, Feb. 2010.

[6] A. A. Akhil, G. Huff, A. B. Currier, B. C. Kaun, D. M. Rastler, S. B. Chen, A. L. Cotter, D. T. Bradshaw, and W. D. Gauntlett, "DOE / EPRI 2013 electricity storage handbook in collaboration with NRECA," Sandia National Laboratories, Albuquerque, NM and Livermore, CA, SAND2013-5131, Jul. 2013.

[7] A. Joseph and M. Shahidehpour, "Battery storage systems in electric power systems," in *Proc. IEEE Power Eng. Soc. General Meeting*, Montreal, QC, Canada, 2006.

[8] D. Bhatnagar, A. Currier, J. Hernandez, O. Ma, and B. Kirby, "Market and policy barriers to energy storage deployment," Sandia National Laboratories, Albuquerque, NM and Livermore, CA, SAND2013-7606, Sep. 2013.

[9] T. Lee and N. Chen, "Optimal capacity of the battery energy storage system in a power system," *IEEE Trans. Energy Convers.*, vol. 8, no. 4, pp. 667–673, Dec. 1993.

[10] C. H. Lo and M. D. Anderson, "Economic dispatch and optimal sizing of battery energy storage systems in utility load-leveling operations," *IEEE Trans. Energy Convers.*, vol. 14, no. 3, pp. 824–829, Sep. 1999.

[11] J. T. Alt, M. D. Anderson, and R. G. Jungst, "Assessment of utility side cost savings from battery energy storage," *IEEE Trans. Power Syst.*, vol. 12, no. 3, pp. 1112–1120, Aug. 1997.

[12] S. Chakraborty, T. Senjyu, H. Toyama, A. Y. Saber, and T. Funabashi, "Determination methodology for optimising the energy storage size for power system," *IET Gener. Transm. Distrib.*, vol. 3, no. 11, pp. 987–999, Nov. 2009.

[13] F. A. Chacra, P. Bastard, G. Fleury, and R. Clavreul, "Impact of energy storage costs on economical performance in a distribution substation," *IEEE Trans. Power Syst.*, vol. 20, no. 2, pp. 684–691, May 2005.

[14] W. A. Omran, M. Kazerani, and M. M. A. Salama, "Investigation of methods for reduction of power fluctuations generated from large grid-connected photovoltaic systems," *IEEE Trans. Energy Convers.*, vol. 26, no. 1, pp. 318–327, Mar. 2011.

[15] X. Wang, D. Mahinda Vilathgamuwa, and S. S. Choi, "Determination of battery storage capacity in energy buffer for wind farm," *IEEE Trans. Energy Convers.*, vol. 23, no. 3, pp. 868–878, Sep. 2008.

[16] X. Wang, M. Yue, E. Muljadi, and W. Gao, "Probabilistic approach for power capacity specification of wind energy storage systems," *IEEE Trans. Ind. Appl.*, vol. 50, no. 2, pp. 1215–1224, Mar. 2014.

[17] Y. Ru, J. Kleissl, and S. Martinez, "Storage size determination for grid-connected photovoltaic systems," *IEEE Trans. Sustain. Energy*, vol. 4, no. 1, pp. 68–81, Jan. 2013.

[18] Y. Yang, H. Li, A. Aichhorn, J. Zheng, and M. Greenleaf, "Sizing strategy of distributed battery storage system with high penetration of photovoltaic for voltage regulation and peak load shaving," *IEEE Trans. Smart Grid*, vol. 5, no. 2, pp. 982–991, Mar. 2014.

[19] C. Abbey and G. Joos, "A stochastic optimization approach to rating of energy storage systems in wind-diesel isolated grids," *IEEE Trans. Power Syst.*, vol. 24, no. 1, pp. 418–426, Feb 2009.

[20] T. K. A. Brekken, A. Yokochi, A. von Jouanne, Z. Z. Yen, H. M. Hapke, and D. A. Halamay, "Optimal energy storage sizing and control for wind power applications," *IEEE Trans. Sustain. Energy*, vol. 2, no. 1, pp. 69–77, Jan. 2011.

[21] B. Hartmann and A. Dan, "Methodologies for storage size determination for the integration of wind power," *IEEE Trans. Sustain. Energy*, vol. 5, no. 1, pp. 182–189, Jan. 2014.

[22] H. Bludszuweit and J. A. Dominguez-Navarro, "A probabilistic method for energy storage sizing based on wind power forecast uncertainty," *IEEE Trans. Power Syst.*, vol. 26, no. 3, pp. 1651–1658, Aug. 2011.

[23] Q. Li, S. S. Choi, Y. Yuan, and D. L. Yao, "On the determination of battery energy storage capacity and short-term power dispatch of a wind farm," *IEEE Trans. Sustain. Energy*, vol. 2, no. 2, pp. 148–158, Apr. 2011.

[24] Y. M. Atwa and E. F. El-Saadany, "Optimal allocation of ESS in distribution systems with a high penetration of wind energy," *IEEE Trans. Power Syst.*, vol. 25, no. 4, pp. 1815–1822, Nov. 2010.

[25] S. X. Chen, H. B. Gooi, and M. Q. Wang, "Sizing of energy storage for microgrids," *IEEE Trans. Smart Grid*, vol. 3, no. 1, pp. 142–151, Mar. 2012.

[26] J. Mitra, "Reliability-based sizing of backup storage," *IEEE Trans. Power Syst.*, vol. 25, no. 2, pp. 1198–1199, May 2010.

[27] J. Mitra and M. R. Vallem, "Determination of storage required to meet reliability guarantees on island-capable microgrids with intermittent sources," *IEEE Trans. Power Syst.*, vol. 27, no. 4, pp. 2360–2367, Nov. 2012.

[28] S. Bahramirad, W. Reder, and A. Khodaei, "Reliability-constrained optimal sizing of energy storage system in a microgrid," *IEEE Trans. Smart Grid*, vol. 3, no. 4, pp. 2056–2062, Dec. 2012.

[29] A. S. A. Awad, T. H. M. EL-Fouly, and M. M. A. Salama, "Optimal ESS allocation and load shedding for improving distribution system reliability," *IEEE Trans. Smart Grid*, vol. 5, no. 5, pp. 2339–2349, Sep. 2014.

[30] Y. V. Makarov, P. Du, M. C. W. Kintner-Meyer, C. Jin, and H. F. Illian, "Sizing energy storage to accommodate high penetration of variable energy resources," *IEEE Trans. Sustain. Energy*, vol. 3, no. 1, pp. 34–40, Jan. 2012.

[31] B. S. Borowy and Z. M. Salameh, "Methodology for optimally sizing the combination of a battery bank and PV array in a wind/PV hybrid system," *IEEE Trans. Energy Convers.*, vol. 11, no. 2, pp. 367–375, Jun. 1996.

[32] E. Koutroulis, D. Kolokotsa, A. Potirakis, and K. Kalaitzakis, "Methodology for optimal sizing of stand-alone photovoltaic/wind-generator systems using genetic algorithms," *Solar energy*, vol. 80, no. 9, pp. 1072–1088, Sep. 2006.

[33] A. R. Prasad and E. Natarajan, "Optimization of integrated photovoltaic–wind power generation systems with battery storage," *Energy*, vol. 31, no. 12, pp. 1943–1954, Sep. 2006.

[34] L. Xu, X. Ruan, C. Mao, B. Zhang, and Y. Luo, "An improved optimal sizing method for wind-solar-battery hybrid power system," *IEEE Trans. Sustain. Energy*, vol. 4, no. 3, pp. 774–785, Jul. 2013.

[35] S. Kahrobaee, S. Asgarpoor, and W. Qiao, "Optimum sizing of distributed generation and storage capacity in smart households," *IEEE Trans. Smart Grid*, vol. 4, no. 4, pp. 1791–1801, Dec. 2013.

[36] P. Yang and A. Nehorai, "Joint optimization of hybrid energy storage and generation capacity with renewable energy," *IEEE Trans. Smart Grid*, vol. 5, no. 4, pp. 1566–1574, Jul. 2014.

[37] W. Su and J. Wang, "Energy management systems in microgrid operations," *The Electricity Journal*, vol. 25, no. 8, pp. 45–60, 2012.

[38] D. E. Olivares, A. Mehrizi-Sani, A. H. Etemadi, C. A. Canizares, R. Iravani, M. Kazerani, A. H. Hajimiragha, O. Gomis-Bellmunt, M. Saeedifard, R. Palma-Behnke, G. A. Jimenez-

Estevez, and N. D. Hatziargyriou, "Trends in microgrid control," *IEEE Trans. Smart Grid*, vol. 5, no. 4, pp. 1905–1919, Jul. 2014.

[39] D. E. Olivares, C. A. Canizares, and M. Kazerani, "A centralized energy management system for isolated microgrids," *IEEE Trans. Smart Grid*, vol. 5, no. 4, pp. 1864–1875, Jul. 2014.

[40] A. L. Dimeas and N. D. Hatziargyriou, "Operation of a multiagent system for microgrid control," *IEEE Trans. Power Syst.*, vol. 20, no. 3, pp. 1447–1455, Aug. 2005.

[41] M. Arriaga, C. A. Canizares, and M. Kazerani, "Renewable energy alternatives for remote communities in northern Ontario, Canada," *IEEE Trans Sustain. Energy*, vol. 4, no. 3, pp. 661–670, Jul. 2013.

[42] N. Hatziargyriou, H. Asano, R. Iravani, and C. Marnay, "Microgrids," *IEEE Power and Energy Magazine*, vol. 5, no. 4, pp. 78–94, Jul. 2007.

[43] D. Curtis and B. M. Singh, "Northern micro-grid project-A concept," in *Proc. World Energy Congress*, Montreal, QC, Canada, 2010.

[44] A. H. Hajimiragha and M. R. Dadash Zadeh, "Research and development of a microgrid control and monitoring system for the remote community of Bella Coola: Challenges, solutions, achievements and lessons learned," in *IEEE Int. Conf. on Smart Energy Grid Eng.*, Aug. 2013.

[45] M. Barnes, J. Kondoh, H. Asano, J. Oyarzabal, G. Ventakaramanan, R. Lasseter, N. Hatziargyriou, and T. Green, "Real-world microgrids-An overview," in *Proc. IEEE Int. Conf. Syst. Syst. Eng.*, Apr. 2007.

[46] P. Grbovic, "Energy storage technologies and devices," in *Ultra-Capacitors in Power Conversion Systems:Analysis, Modeling and Design in Theory and Practice*. Wiley-IEEE Press, 2014, pp. 1–21.

[47] T. Kousksou, P. Bruel, A. Jamil, T. El Rhafiki, and Y. Zeraouli, "Energy storage: Applications and challenges," *Solar Energy Materials and Solar Cells*, vol. 120, pp. 59–80, Jan. 2014.

[48] P. B. V. Viswanathan, M. Kintner-Meyer and C. Jin, "National assessment of energy storage for grid balancing and arbitrage: Phase 2, Volume 2: Cost and performance characterization," Pacific Northwest National Laboratory, Richland, WA, PNNL-21388, Sep. 2013.

[49] J. Leadbetter and L. G. Swan, "Selection of battery technology to support grid-integrated renewable electricity," *Journal of Power Sources*, vol. 216, pp. 376–386, Oct. 2012.

[50] M. Beaudin, H. Zareipour, A. Schellenberglabe, and W. Rosehart, "Energy storage for mitigating the variability of renewable electricity sources: An updated review," *Energy for Sustainable Development*, vol. 14, no. 4, pp. 302–314, Dec. 2010.

[51] G. B. Sheble and G. N. Fahd, "Unit commitment literature synopsis," *IEEE Trans. Power Syst.*, vol. 9, no. 1, pp. 128–135, Feb. 1994.

[52] N. P. Padhy, "Unit commitment-A bibliographical survey," *IEEE Trans. Power Syst.*, vol. 19, no. 2, pp. 1196–1205, May 2004.

[53] L. Wu, "A tighter piecewise linear approximation of quadratic cost curves for unit commitment problems," *IEEE Trans. Power Syst.*, vol. 26, no. 4, pp. 2581–2583, Nov. 2011.

[54] M. Carrion and J. M. Arroyo, "A computationally efficient mixed-integer linear formulation for the thermal unit commitment problem," *IEEE Trans. Power Syst.*, vol. 21, no. 3, pp. 1371–1378, Aug. 2006.

[55] A. M. Zein Alabedin, E. F. El-Saadany, and M. M. A. Salama, "Generation scheduling in microgrids under uncertainties in power generation," in *IEEE Electrical Power and Energy Conf.*, 2012.

[56] A. H. Hajimiragha, M. R. Dadash Zadeh, and S. Moazeni, "Microgrids frequency control considerations within the framework of the optimal generation scheduling problem," *IEEE Trans. Smart Grid*, vol. 6, no. 2, pp. 534–547, Mar. 2015.

[57] F. Ramos-gaete, "Modeling and analysis of price-responsive loads in the operation of smart grids," Master's thesis, University of Waterloo, Waterloo, ON, Canada, 2013.

[58] A. Y. Saber and G. K. Venayagamoorthy, "Resource scheduling under uncertainty in a smart grid with renewables and plug-in vehicles," *IEEE Syst. Journal*, vol. 6, no. 1, pp. 103–109, Mar. 2012.